***Referee's Comment in Italic Font;* Author's response in Blue without Italic Font.**

Response to Referee #1

(1) Lines 24-26, page 31154. Information on the total concentration of aromatic hydrocarbons with more than three methyl groups would be necessary.

Ambient concentrations of aromatics with more than three methyl groups is scarce. Nevertheless, aromatic hydrocarbons with more than three methyl groups contributes to a large portion of components in products such as gasoline and crude oil (Diehl, et al., 2005; Darouich, et al., 2006). Therefore, we insert "Aromatic hydrocarbons with more than three methyl groups contributes to a large portion of components in products such as gasoline and crude oil (Diehl, et al., 2005; Darouich, et al., 2006)" at Lines 26, page 31154 before "Moreover"

(2) Lines 12-14, page 31155. What is the definition of "methyl group branching ratio"? The terminology, "branching ratio", is often used for product branching ratio and would make readers confused.

Good point. We replace "methyl group branching ratio" with "the increase of branched structure".

(3) Lines 17-18, page 31155. The expression, "aliphatic hydrocarbons", should be substituted with "alkane and alkene hydrocarbons" because Sato et al. (2011) reported that the SOA yield from aliphatic dinene compounds are found to decrease with increasing the number of methyl side chains.

Agreed. We replace "aliphatic hydrocarbons" with "alkane and alkene hydrocarbons".

(4) Line 27, page 31158 – line 1, page 31159. The authors discuss on the results of product volatility parameter based on gas-particle partitioning model; however the authors conclude in the latter part of manuscript that particle-phase oligomerization plays important roles during SOA formation. Particle-phase oligomerization is not taken into account for the gas-partitioning model. Trump and Donahue (2014) reported that formation of oligomer-containing SOA particles can be interpreted by gas-particle partitioning model only if oligomer formation is reversible; however, present experimental results do not contain any evidences showing that oligomer formation is reversible. The product volatility parameters obtained by present fitting would not have physical meaning which is defined by the gas-particle partitioning model.

True. We change the sentence "The more volatile parameters ($K_{om,2}$) are similar for all yield curve fits, suggesting that compounds of similar gas-particle partitioning parameters are formed from the photooxidation of all aromatic hydrocarbons studied." to "The higher-volatility partitioning parameter ($K_{om,2}$) in all yield curve fitting are assigned to a fixed value by assuming similar high volatile compounds are formed during all aromatic hydrocarbon photooxidation experiments."

Further, per the Trump and Donahue (2014) reference, it is suggested in that paper that

reversible oligomerization is required to obtain low aerosol yields at low mass loadings consistent with the aerosol yields observed in this paper.

(5) Line 21, page 31159. Does "the methyl group number effect" mentioned here indicate the effect of methyl group number on SOA yield?

Yes. We make the following change is suggested to improve clarity. We change "that the methyl group number effect is greater than the effect of increasing k_{OH}" into "the effect of methyl group number on SOA yield is greater than that of the increasing k_{OH} on SOA yield, which is related to aromatic hydrocarbon oxidation process."

(6) Line 6, page 31161. The readers who do not belong to AMS community might not be familiar to "the AMS frag Table of Unit Resolution Analysis."

It is possible that reader is not familiar with AMS frag Table of Unit Resolution Analysis. Therefore, we insert "which describes the mathematical formulation of the apportionment at each unit resolution sticks to aerosol species" after "the AMS frag Table of Unit Resolution Analysis".

(7) Lines 17-21, page 31170. As described in comment (6), product volatility parameters should carefully be interpreted when particle-phase oligomerizations play important roles during SOA formation.

Thanks for the suggestion. In this study, we are not sure about the reversibility of the oligomerization that occurs during the photooxidation of aromatic hydrocarbons. However, a reversible oligomerization process is suggested by Trump and Donahue, 2014. We insert "especially at higher particle mass loadings" after line 19 "than oligomerization products (S_2)". We also insert "by assuming the oligomerization process may be a reversible process (Trump and Donahue, 2014)" at the end of this sentence (Line 21) to make the discussion part more reasonable.

(8) Lines 2-7, page 31171. The authors describe that methyl groups inhibit oligomerization; however, ketones could proceed to aldol condensation and hemiacetal formation (Jang et al., 2002). For readers' understanding, further explanations would be necessary.

It is a good point. Additional discussion is added in the manuscript. We insert the following sentence after "when methyl groups are attached to both ends of an unsaturated dicarbonyl" at line 7 page 31171: "Oligomerization is possible for these ketones through reactions such as aldol condensation and hemiacetal formation (Jang et al., 2002) under acidic conditions. However, this is less favored for the current study in the absence of acidic seeds."

(9) Page 31189, Fig. 1. The curves of tetramethylbenzene and C10+ are extrapolated beyond the region of experimental data points. Extrapolated curves should be deleted.

We agree and the extrapolation is deleted (New Figure 1 uploaded).

(10) The caption of Table S1. What kind of approximation method was used for the prediction of the pentamethylbenzene vapor pressure?

Good catch. Actually, the value "3.48e-2" is an experimental data for pentamethylbenzene vapor pressure at 20 degree C, which can be found in the Chemspider line below

http://www.chemspider.com/Chemical-Structure.12259.html?rid=925ba290-a294-41e2-b8c5-346c0d3124f1. The vapor pressure listed in our paper is from the same vapor pressure source as other aromatic hydrocarbons, which is thereby comparable. However, "*" should be noted as "Experimental vapor pressure measured at 20°C, An estimated vapor pressure at 25°C is 3.56e-2 according to Chemispider" instead of "*Predicted data from Chemispider".

(11) Table S2. HC/NO ratio data would be incorrect. For example, HC concentration in experiment 104A is 2,800 ppbC (= 350 (ppb) x 8 (C atmos)) and NO concentration is 64.4 ppb; therefore HC/NO ratio should be 43.5 ppbC/ppb (=2,800/64.4).
Good catch. HC concentration listed in Table S2 is in a unit of (ug/m3). Correction is made to these values.

Technical comments:
(12) Line 7, page 31158. "Table 2" should be "Table 2S".
Good point. Corrected. Table 2 to Table S2.

(13) Line 27, page 31158. The expression, "the more volatile parameters (Kom, 2)", should be substituted with "higher-volatility partitioning parameter (Kom,2)" for readers' understanding.
Agree. Changed all into "higher-volatility partitioning parameter ($K_{om,2}$)".

(14) Line 24, page 31166. "H2O" should be "H2O+"
Fixed.

(15) Line 19, page 31170. "Oligomerization products (S2)" should be "oligomerization products (S3)".
Fixed.

Response to Referee #2

1-page 31153, In title and in many places throughout article it would be more accurate to say "monocyclic aromatic hydrocarbons" instead of the more general "aromatic hydrocarbons" to make clear that the focus of this study was benzene and substituted benzene compounds.

Agree. We will change all "aromatic hydrocarbons" to "monocyclic aromatic hydrocarbons".

2-page 31154, line 2, The wording "determines the SOA formation" is unclear. Does it refer to SOA yield? composition? Both?

The "SOA formation" means both the SOA yield and SOA chemical composition. We will insert "(SOA yield and chemical composition)" after "determines the SOA formation".

3-page 31154, line 16, Unclear what is meant by "less oxidized per mass/carbon."

"less oxidized per mass/carbon" corresponds to two parameters which are used to compare the SOA formation difference in different aromatic hydrocarbons in this paper. "oxidized per mass" refers to SOA yield which determines SOA formation potential on a mass basis. "oxidized per carbon" refers to SOA chemical composition (e.g. OSc, O/C and H/C) which determines SOA formation potential on a mole or carbon number basis. To clarify the meaning of "less oxidized per mass/carbon", we will add "on a basis of SOA yield or chemical composition" after "less oxidized per mass/carbon".

4-page 31155, line 13, Define what is meant by "methyl group branching"

Good point. We will replace "methyl group branching ratio" with "the increase of branched structure".

5-page 31158, line 14, How are the yield values found in this study different from those in previous studies? Higher or lower?

The differences in absolute values of SOA yield in previous studies and this studies depend on the photooxidation conditions. For example, earlier work (Odum et al., 1997b; Kleindienst et al., 1999; Cocker et al., 2001b; Sato et al., 2012) observed much lower SOA yield than this study due to the higher NO_x conditions in these earlier work. Ng et al. (2007) observed similar SOA yields to this study under low NO_x conditions with seed added before photooxidation. Nevertheless, this study focuses on the SOA yield difference among aromatic hydrocarbons with difference number of methyl substitutes on aromatic ring. We found the SOA yield trend in this work agrees with previous studies.

6-page 31158, line 17, How much higher are the current benzene SOA yields compared to the cited studies?

Current benzene SOA yield are more than two times higher than the cited studies under similar mass loadings. Borrás and Tortajada-Genaro(2012) and Martín-Reviejo and Wirtz (2005) use natural light which might cause some fluctuation in light intensity, temperature and other

conditions and therefore affect SOA yield. Sato et al (2012) provided only one data point under low NOx condition at a comparatively low mass loadings (18 ug/m^3) under different light source (19 Xe arc lamp) compared with this study.

7-page 31159, line 11, Change "suppresses SOA formation" to "suppresses formation of lower volatility products"
Agree. We will fix it.

8-page 31159, lines 12-14, The claim in this sentence has not yet been supported. Perhaps change "indicates" to "suggests"
Agree. We will fix it.

9-page 31159, lines 25-26, Possibility (3) seems to be just an observation of behavior, not an explanation for the methyl group effect.
Agree. We will change "three" possibilities to "two". We will replace ";" before "(3)" with "." Replace possibility (3) with the following sentence "Therefore, the methyl group increases hydrocarbon mass consumption more than particle mass formation".

10-page 31159, line 29, SOA yields at what point in the experiment? Yield varies with time/Mo/deltaHC so it is important to specify what yield values are being used for the correlation.
Agree. We will replace "average radical parameter" at *page 31159, line 29* with "average radical concentrations throughout photooxidation". The SOA yield we used is the final SOA yield at the end of the photooxidation. This work uses "average radical concentrations throughout photooxidation" and "average radical concentrations are calculated by dividing time integrated radical parameters with photooxidation time" as mentioned in Table S3. Therefore, the time and deltaHC are considered in the "average radical concentrations". Most SOA yield are under comparable mass loading (M_o<60 ug/m^3) and the few large mass loading points should not dramatically the overall relationships we found.

11-page 31160, line 2, OH is the only parameter with a statistically significant correlation (p<0.05). The strength of correlation values for all the other parameters are meaningless since the relationships aren't statistically significant.
Agree. Replace "the best correlated parameter" with "the only parameter investigated with a statistically significant correlation (p<0.05)".

12-page 31160, line 15, Add a sentence explaining what f44 and f43 represent relative to degree of oxidation.
We will add "A higher f_{44} and a lower f_{43} indicates a higher degree of oxidation (Ng et al., 2010, 2011)." before "The f_{44} and f_{43} evolution" at page 31160, line 15.

13-page 31160, line25, Explain what is meant by "evolution trend". Also, tetramethylbenzene seems to shift too.
Good point. We will add "and tetramethylbenzene" after "*m*-xylene" and will delete "and" before

"*m*-xylene". We will also add "Evolution of SOA composition (Heald, et al., 2009; Jimenez, et al., 2009) refers to SOA chemical composition changes with time and f_{44} and f_{43} evolution refers to the change of f_{44} and f_{43} with time" before the "Significant f_{44} and f_{43} evolution" and delete "trend" after "evolution" at line25 page 31160.

14-page 31161, line 1, Here and throughout the article it refers to general trends of parameters increasing or decreasing with the number of methyl groups. It would be helpful to make clear that it is not a uniform or consistent trend. For example, in Figure 2 the number of methyl groups is in the order 0,1,2,3,5,4,6, while in Figure 3a it is 0,1,3,2,4,6,5.

Agree. The slight difference in the order is due to the isomer impact on the chemical composition and yield, which is addressed in Li, et al (2016) (another paper submitted to ACP). We will add "It should also be noticed that the higher O/C and lower H/C observed in SOA formed from 1,2,4-trimethylbenzne (three methyl substitute aromatic hydrocarbon) than that from *m*-xylene (two methyl substitute aromatic hydrocarbon) is due to the isomer impact on SOA chemical composition, which is discussed in details by Li, et al (2015)." at line 25 on page 31162 after "SOA yield is dependent on SOA chemical composition"

15-page 31162, line 11, What is the "elemental ratio evolution trend" and how does it agree with the f44 vs f43 trend?

The elemental ratio evolution is defined similarly to f_{44} vs. f_{43} evolution. We will add "The change of elemental ratio (H/C and O/C) with time is referred as elemental ratio evolution." before "The elemental ratio evolution trend agrees with the f_{44} vs. f_{43} trend." and replace "evolution trend" and "trend" with "evolution" in this sentence. We will add "(significant evolution in benzene and slightly for toluene, m-xylene and 1,2,4,5-tetramethylbenzene)" in the end of the sentence "The elemental ratio evolution agrees with the f_{44} vs. f_{43}" in order to clarify the point that the similarity of the two chemical evolution is about how significant the chemical evolution is during the SOA formation from each aromatic precursor.

16-page 31164, line 16, Only m-xylene results are reported. Would there be differences for the other xylenes (o-xylene, p-xylene)? Similarly for the tri- and tetra- methylbenzenes.

Good point. We have a detailed analysis on isomer structure impact (three different xylenes and three different trimethylbenzenes) on SOA chemical composition which can be found in Li et al.(2016).

17-page 31164, line 23, Pentamethylbenzene also shows a significant overestimation and should be mentioned.

Agree. We will insert in the end of line 4 page 31165 "It is also noticed that O/C and OS_c is slightly overestimated in SOA formed from pentamethylbenzene. This indicates that the methyl group hindrance impact on aromatic hydrocarbon oxidation should be explained by multiple pathways which have different impact on SOA formation."

18-page 31166, line 14, Density underestimation doesn't seem to "enlarges with increasing methyl group", but appears about the same for 2,3,4,5 methyl groups. And should also mention,

and possibly discuss, the overprediction for benzene and toluene.

Agree. The underestimation is not monotonically increasing with the number of methyl group since similar products are expected to form even with the increase of methyl group as mentioned in Disucssion 4.1. We will focus more on the general trend of the difference between density prediction and measurement while more methyl groups are attached to aromatic ring.

page 31166, line 14: We will replace "SOA density underestimation enlarges with increasing methyl group number" with "SOA density difference between prediction and measurement change from positive (0&1 methyl group) to negative (2,3,4 or 5 methyl groups) with increasing methyl group number."

31167 line 1: We will replace "where a larger negative error is seen as the number of methyl groups increases" with "where a change of error from positive to negative is seen as the number of methyl groups change from less than two to two or more than two "

Hence, the overprediction for benzene and toluene is also mentioned discussed.

19-page 31172, line 6, Change "A decreasing trend" to "A generally decreasing trend"

Agree. We will fix it.

20-page 31172,line 10, Clarify what is meant by "aromatic aging". Aging can refer to many different changes. The statement would be correct if it defines aging as transformation to less volatile compounds.

Agree. We will replace "aromatic aging" with "the oxidation of aromatic hydrocarbon to less volatile compounds".

21-page 31172, lines 15-16, Are benzene and toluene always the most important precursors of those studied here? Or is it just under low NOx conditions?

This study confirms the importance of benzene and toluene to the SOA formation among all aromatic hydrocarbon under low NO_x conditions. Earlier work on SOA formation from aromatic hydrocarbons suggest that benzene and toluene are dominating SOA precursors under high NO_x and NOx free conditions (Odum, et al., 1997; Takekawa, et al., 2003; Ng, et al., 2007; Borrás and Tortajada-Genaro,2012). The key point that low NO_x conditions are much more atmospherically relevant than high NO_x conditions and therefore benzene and toluene are critical aromatic precursors for SOA formation especially in urban areas.

22-page 31172, lines 17-19, Hexamethylbenzene is not the only compound with a discrepancy between predicted and measured oxidation, calling into question the claim of uniqueness. Both m-xylene and pentamethylbenzene are much less oxidized than predicted.

We agree that we also observed discrepancy between prediction and measurement in the oxidation of *m*-xylene and pentamethylbenzene. However, only hexamethylbenzene is more oxidized than the prediction and *m*-xylene and pentamethylbenzene are less oxidized than the prediction. The lower oxidation of *m*-xylene than the prediction is associated with the xylene isomer impact on SOA formation and chemical composition which is further discussed in Li, et al (2016) ACPD paper. The lower oxidation of pentamethylbenzene than the prediction is explained by the methyl group hindrance on oxidation. What is unique in hexamethylbenzene is that the

oxidation is higher than the prediction even with maximum methyl group hindrance possibility. The slight H/C decrease in Fig 3b and the underestimation in OSc and O/C all support the uniqueness of hexamethylbenzene.

Technical Corrections:

23-page 31158, line 7, Should "(Table 2)" read "(Table S2)"?

Good point. Corrected.

24-page 31164, lines 14-15, add "_SOA" to subscripts for "O/Cpre,i" and "H/Cpre,i" to make clear it is the elemental ratio of SOA, not of the precursor.

Agree. We will change "$O/C_{pre,i}$" and "$H/C_{pre,i}$" to "$O/C_{pre,i\_SOA}$" and "$H/C_{pre,i\_SOA}$".

25-page 31165, line 7, The R2 correlation values listed in the text seem too high for the data shown in Figure S3.

Good point. We will replace "R^2" with "Pearson correlation".

26-page 31167, line 8, Define VFR the first time the acronym is used.

Agree. We should be consistent with the terminology we use. In page 31157, line 12, we will replace "Volume remaining fraction (VRF)" with "Volume fraction remaining (VFR)".

27-page 31168, lines 4-5, Correlation coefficients and p-values listed in the text are not the same as those in Table S5.

Fixed. Replace "O/C (0.932, p = 0.02) and OSc (0.931, p = 0.002)" with "O/C (0.937, p = 0.002) and OSc (0.932, p = 0.02)".

28-pages 31190-31191, The coloring in Figures 2 and 3 that corresponds to the number of methyl groups would be much more useful if it was consistent. In Figure 2 and Figure 3a the colors for 0/1/2/3/4/5/6 methyl groups appears to be red/yellow/green/light blue/dark blue/orange/gray (but with purple dots for 5 and 6). In Figure 3b, however, the colors are red/orange/green/green/light blue/dark blue/purple.

Thanks for suggestion. We will change Figure 3b color to match the colors in Figure 2 and Figure 3a. See below for the update in Figure 3b color. We keep the dashed line between toluene precursor and SOA as orange since yellow is too bright to show clearly in a white background.

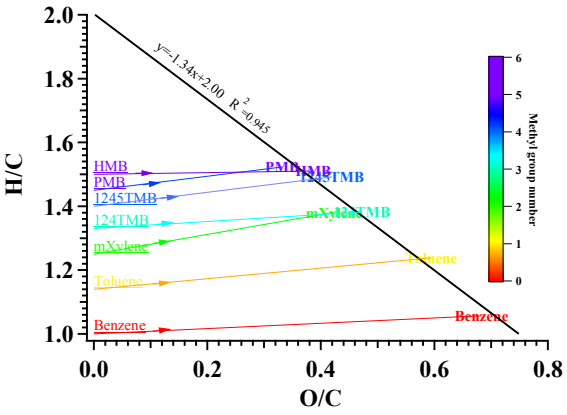

Other relevant changes made in the manuscript

1. Figure 7 replace “benzene shown as an example” with “methyl substitute on aromatic ring not shown”
2. Correct the amount of aromatic hydrocarbon precursors into “seven” instead of “six” (Page 31158 Line 3, Line 9)
3. Insert following reference to the list

   Darouich, T. AI., Behar, F. and Largeau., C.: Thermal cracking of the light aromatic fraction of Safaniya crude oil–experimental study and compositional modelling of molecular classes. Org. Geochem., 37(9), 1130-1154, doi:. 10.1016/j.orggeochem.2006.04.003, 2006

   Diehl, J. W. and Sanzo, F. P. Di.: Determination of aromatic hydrocarbons in gasolines by flow modulated comprehensive two-dimensional gas chromatography, J. Chromatogr. A., 1080(2): 157-165, doi:10.1016/j.chroma.2004.11.054, 2005.

Role of methyl group number on SOA formation from monocyclic aromatic hydrocarbons photooxidation under low NO_x conditions

L. Li[1,2], P. Tang[1,2], S. Nakao[1,2,3], C-L. Chen[1,2,4] and D. R. Cocker III[1,2]

[1] University of California, Riverside, Department of Chemical and Environmental Engineering, Riverside, CA 92507, USA

[2] College of Engineering-Center for Environmental Research and Technology (CE-CERT), Riverside, CA 92507, USA

[3] Currently at Clarkson University, Department of Chemical and Biomolecular Engineering, Potsdam, NY 13699, USA

[4] Currently at Scripps Institution of Oceanography, University of California, La Jolla, California, USA

Correspondence to: D. Cocker III (dcocker@engr.ucr.edu)

Abstract

Substitution of methyl groups onto the aromatic ring determines the SOA formation from the monocyclic aromatic hydrocarbon precursor (SOA yield and chemical composition). This study links the number of methyl groups on the aromatic ring to SOA formation from monocyclic aromatic hydrocarbons photooxidation under low NO_x conditions (HC/NO>10 ppbC:ppb). Monocyclic ~~Aromatic~~ aromatic hydrocarbons with increasing numbers of methyl groups are systematically studied. SOA formation from pentamethylbenzene and hexamethylbenzene are reported for the first time. A decreasing SOA yield with increasing number of methyl groups is observed. Linear trends are found in both f_{44} vs. f_{43} and O/C vs. H/C for SOA from monocyclic aromatic hydrocarbons with zero to six methyl groups. An SOA oxidation state predictive method based on benzene is used to examine the effect of added

methyl groups on aromatic oxidation under low NO_x conditions. Further, the impact of methyl group number on density and volatility of SOA from monocyclic aromatic hydrocarbons is explored. Finally, a mechanism for methyl group impact on SOA formation is suggested. Overall, this work suggests as more methyl groups are attached on the aromatic ring, SOA products from these monocyclic aromatic hydrocarbons become less oxidized per mass/carbon on a basis of SOA yield or chemical composition.

Key Words: Monocyclic ~~Aromatic~~ aromatic hydrocarbons; Anthropogenic sources; SOA density; SOA composition; Aging; SOA yield

1. Introduction

Aromatic hydrocarbons are major anthropogenic SOA precursors (Kanakidou, et al., 2005; Henze, et al., 2008). Monocyclic ~~Aromatic~~ aromatic hydrocarbons with less than four methyl groups are ubiquitous in the atmosphere (Singh et al., 1985; Singh et al., 1992; Fraser, et al., 1998; Pilling and Bartle, 1999; Holzinger, et al., 2001; Buczynska, et al., 2009; Hu et al., 2015). Monocyclic ~~Aromatic~~ aromatic hydrocarbons with more than 4 methyl groups are barely investigated in previous ambient studies, possibly due to a vapor pressure decrease with carbon number (Pankow and Asher, 2008; Table S1). However, a recent study observed that compounds with low vapor pressure are available to evaporate into the atmosphere (Võ and Morris, 2012). Monocyclic aromatic hydrocarbons with more than three methyl groups contributes to a large portion of components in products such as gasoline and crude oil (Diehl, et al., 2005; Darouich, et al., 2006). Moreover, hydrocarbon reactivity and OH reaction rate constant (k_{OH}) increase with methyl group number (k_{OH} Table S1; Glasson, et al., 1970; Calvert, et al, 2002; Atkinson and Arey, 2003; Aschmann, et al, 2013). OH-initiated reactions, particularly OH addition to the aromatic ring, dominate aromatic photooxidation (Calvert, et al., 2002). Hence, photooxidation occurs rapidly once these low vapor pressure aromatic hydrocarbons evaporate into atmosphere. In addition, an increase in carbon number is associated

with a decrease in vapor pressure (Pankow and Asher, 2008). Higher carbon number products with a similar amount of functional groups have a higher tendency to participate in the particle phase. However, aging of organic aerosol is a combination of functionalization, fragmentation and oligomerization (Jimenez, et al., 2009; Kroll, et al., 2009). Therefore, rapid aging does not necessarily lead to the highly oxidized compounds, which serve as an important source of SOA.

Recent studies have found that SOA yields from OH initiated alkane and alkene reactions increase with carbon chain length and decrease with the increase of branched structure ~~methyl group branching ratio~~ (Lim, and Ziemann, 2009; Matsunaga, et al., 2009; Tkacik, et al., 2012). However, SOA yield from monocyclic aromatics are found to decrease with carbon number by adding methyl groups to the aromatic ring (Odum, et al., 1997; Cocker, et al., 2001b; Sato, et al., 2012). This indicates that the role of methyl groups on the aromatic ring is different than for alkane and alkene hydrocarbons~~aliphatic hydrocarbons~~. Previous studies show that the relative methyl group position determines the alkoxyl radical (RO·) fragmentation ratio in ~~aliphatic~~ alkane and alkene hydrocarbon~~hydrocarbon~~ oxidation (Atkinson, 2007; Ziemann, 2011). Therefore, it is necessary to explore the impact of methyl groups on SOA formation during monocyclic aromatic hydrocarbon oxidation.

Previous studies on SOA formation from monocyclic aromatic hydrocarbon in the presence of NO_x have been conducted at high NO_x levels (e.g., Odum, et al., 1997; Cocker, et al., 2001b; Sato, et al., 2012). Ng, et al (2007) observed that SOA yield decreases with increasing carbon number under high NO_x conditions and no trends were observed for no NO_x conditions. Reaction mechanisms vary for different NO_x conditions (e.g., Song, et al., 2005; Kroll and Seinfeld, 2008) and thus impact SOA chemical composition. Therefore, it is necessary to investigate methyl group impact on urban SOA formation from monocyclic aromatic hydrocarbon under more atmospherically relevant low NO_x conditions.

SOA budget underestimation of the urban environment is associated with mechanism uncertainty in aromatic hydrocarbon photooxidation and possibly missing aromatic hydrocarbon precursors (Henze, et al., 2008; Hallquist, et al., 2009). Previous chamber studies seldom investigate SOA formation from monocyclic aromatic with more than 3 methyl groups (e.g. pentamethylbenzene and hexamethylbenzene). This study investigates SOA formation from the photooxidation of seven monocyclic aromatic hydrocarbon (ranging from benzene to hexamethylbenzene) under the low NO_x (HC/NO>10 ppbC:ppb) condition. The impact of methyl group number on SOA yield, chemical composition and other physical properties are demonstrated. Possible methyl group impact on aromatic ring oxidation, decomposition and subsequent oligomerization are discussed.

2. Method

2.1 Environmental chamber

All experiments were conducted in the UC Riverside/CE-CERT indoor dual 90 m^3 environmental chambers, which are described in detail elsewhere (Carter et al., 2005). All experiments were conducted at dry conditions (RH<0.1%), in the absence of inorganic seed aerosol and with temperature controlled to 27±1°C. Two movable top frames were slowly lowered during each experiment to maintain a slight positive differential pressure (~0.02" H_2O) between the reactors and enclosure to minimize dilution and/or contamination of the reactors. 272 115 W Sylvania 350BL blacklights are used as light sources for photooxidation.

A known volume of high purity liquid hydrocarbon precursors (benzene Sigma-Aldrich, 99%; toluene Sigma-Aldrich, 99.5%; *m*-xylene Sigma-Aldrich, 99%; 1, 2, 4-trimethylbenzene Sigma-Aldrich, 98%) were injected through a heated glass injection manifold system and flushed into the chamber with pure N_2. A glass manifold packed with glass wool inside a temperature controlled oven (50-80 °C) is used to inject solid hydrocarbon precursors (1, 2, 4, 5-tetramethylbenzene

Sigma-Aldrich, 98%; pentamethylbenzene Sigma-Aldrich, 98%; hexamethylbenzene Sigma-Aldrich, 99%). NO was introduced by flushing pure N_2 through a calibrated glass bulb filled to a predetermined partial pressure of pure NO. All hydrocarbons and NO are injected and well mixed before the lights were turned on to commence the reaction.

2.2 Particle and Gas Measurement

Particle size distribution between 27 nm and 686 nm was monitored by dual custom built Scanning Mobility Particle Sizers (SMPS) (Cocker et al., 2001a). Particle effective density was measured with a Kanomax Aerosol Particle Mass Analyzer (APM-SMPS) system (Malloy et al., 2009). Particle volatility was measured by a Volatility Tandem Differential Mobility Analyzer (VTDMA) (Rader and McMurry, 1986) with a Dekati® Thermodenuder controlled to 100°C and a 17 s heating zone residence time (Qi, et al., 2010b). Volume fraction remaining (VFR)~~Volume remaining fraction (VRF)~~ is calculated as $(D_{p,\text{ after TD}}/D_{p,\text{ before TD}})^3$.

Evolution of particle-phase chemical composition was measured by a High Resolution Time of Flight Aerosol Mass Spectrometer (HR-ToF-AMS; Aerodyne Research Inc.) (Canagaratna et al., 2007; DeCarlo et al., 2006). The sample was vaporized by a 600 °C oven followed by a 70 eV electron impact ionization. f_x in this study is calculated as the fraction of the organic signal at *m/z*=x. For example, f_{44} and f_{43} are the ratios of the organic signal at *m/z* 44 and 43 to the total organic signal, respectively (Chhabra et al., 2011; Duplissy et al., 2011). Elemental ratios for total organic mass, oxygen to carbon (O/C), and hydrogen to carbon (H/C) were determined using the elemental analysis (EA) technique (Aiken et al., 2007, 2008). Data was analyzed with ToF-AMS analysis toolkit squirrel 1.56D /PIKA 1.15D version.

The Agilent 6890 Gas Chromatograph – Flame Ionization Detector was used to measure aromatic hydrocarbon concentrations. A Thermal Environmental Instruments Model 42C chemiluminescence NO analyzer was used to monitor NO, NO_y-NO and

NO_y. The gas-phase reaction model SAPRC-11 developed by Carter and Heo (2012) was utilized to predict radical concentrations (·OH, HO_2·, RO_2· and NO_3·).

3. Results

3.1 SOA yield relationship with methyl group number

SOA yields from the photooxidation of ~~six~~seven monocyclic aromatic hydrocarbons are calculated as the mass based ratio of aerosol formed to hydrocarbon reacted (Odum, et al., 1996). The HC/NO ratio ranged from 12.6-110 ppbC:ppb for all experiments used in this study. Experiment conditions and SOA yield are listed from the current work (Table 1) along with additional *m*-xylene experiment conditions from previous studies (Table S2) (Song, et al, 2005) in the UCR CE-CERT chambers. SOA yield as a function of particle mass concentration (M_0) for all ~~six~~ seven monocyclic aromatic precursors (Fig.1) includes experiments listed in both Table 1 and Table S2. Each individual experiment is marked and colored by the number of methyl groups on each precursor aromatic ring. It is observed that SOA yield decreases as the number of methyl groups increases (Fig. 1). A similar yield trend is also observed in previous studies on SOA formation from monocyclic aromatic hydrocarbons, however, different absolute yield values are found, presumably due to higher NO_x levels (Odum, et al., 1997b; Kleindienst et al., 1999; Cocker et al., 2001b; Takekawa et al., 2003; Ng, et al., 2007; Sato, et al., 2012). SOA yields of benzene under comparable low NO_x conditions are higher than that in Sato, et al (2012), Borrás and Tortajada-Genaro (2012) and Martín-Reviejo and Wirtz (2005).

The two product semi-empirical model described by Odum, et al. (1996) is used to fit SOA yield as a function of M_0. Briefly, the two product model assumes that aerosol forming products can be lumped into lower and higher volatility groups whose mass fraction is defined by α_i and a partitioning parameter $K_{om,i}$ ($m^3 \cdot \mu g^{-1}$) described extensively in Odum, et al. (1996). Each monocyclic aromatic hydrocarbon is fitted individually except for those with methyl group number greater than or equal to 4,

which are grouped as C_{10+}. The experimental fitting parameters (α_1, $K_{om,1}$, α_2 and $K_{om,2}$ in Table 2) in the two product model were determined by minimizing the sum of the squared of the residuals. The higher-volatility partitioning parameter parameter ($K_{om,2}$) in all yield curve fitting are assigned to a fixed value by assuming similar high volatile compounds are formed during all monocyclic aromatic hydrocarbon photooxidation experiments~~The more volatile parameters ($K_{om,2}$) are similar for all yield curve fits, suggesting that compounds of similar gas-particle partitioning parameters are formed from the photooxidation of all aromatic hydrocarbons studied~~. Benzene has much higher mass-based stoichiometric coefficients (α_2) than the other monocyclic aromatic compounds indicating that the pathway leading to higher volatility products formation is favored. The lower volatility partitioning parameters ($K_{om,1}$) vary widely for each monocyclic aromatic yield fitting curve. Benzene has the lowest $K_{om,1}$, toluene has the highest $K_{om,1}$, and the rest of monocyclic aromatics have similar mid-range $K_{om,1}$ values. The extremely low $K_{om,1}$ of benzene indicates that pathways associated with significant volatility decrease occur far less during benzene photooxidation than for monocyclic aromatic compounds with methyl groups. Further, $K_{om,1}$ is much lower in multi-methyl group monocyclic aromatic hydrocarbons (with the exception of toluene) while α_1 decreases with methyl group number. This suggests that increasing methyl group number on the aromatic ring suppresses formation of lower volatility products~~SOA formation~~ therefore lowering the mass based aerosol yield. This ~~indicates~~ suggests that monocyclic aromatics with more methyl groups are less oxidized per mass since the methyl group carbon is not well oxidized compared with the ring carbon.

The aromatic SOA growth curves (particle concentration M_0 vs. hydrocarbon consumption ΔHC) under similar HC/NO_x are shown in Fig. S1. The slope of the growth curve is negatively correlated with the parent aromatics reaction rate (k_{OH}). This observation contrasts with a previous study that observed positive correlation between SOA formation rate and hydrocarbon reaction rate for systems where initial semivolatile products dominate gas-particle phase partitioning (Chan, et al., 2007).

Formatted: Subscript

Formatted: Font: (Default) Times New Roman, (Asian) SimSun, 12 pt

The reverse relationship observation in this study indicates that the effect of methyl group number on SOA yield is greater than that of the increasing k_{OH} on SOA yield~~the methyl group number effect is greater than the effect of increasing k_{OH}~~. There are ~~three~~ two possibilities for the methyl group number effect: 1) the methyl group facilitates initial semivolatile products to react into more volatile compounds; 2) the methyl group prevents further generation semivolatile products formation by stereo-hindrance~~;~~. Therefore, ~~3)~~ the methyl group increases hydrocarbon mass consumption more than particle mass formation.

Formatted: Subscript

The relationship between radical levels and SOA yield was also analyzed. Table S3 lists modeled individual ~~average radical parameter~~average radical concentrations throughout photooxidation while Table S4 lists the correlation between SOA yields and individual average radical concentrations. None of the radical parameters (e.g. $\cdot OH/HO_2\cdot$, $HO_2\cdot/RO_2\cdot$ etc.) is strongly correlated with SOA yield. Average OH radical concentration is the only parameter investigated with a statistically significant correlation ($p<0.05$)~~the best correlated parameter~~, as k_{OH} varies with aromatic species and lower average OH concentrations are present with higher k_{OH}. Fig. S2 shows the time evolution of $[\cdot OH]$, $[RO_2\cdot]$ and $[HO_2\cdot]$ for different aromatic precursors under similar initial aromatic and NO_x loadings. Higher $[\cdot OH]$ is observed for aromatic precursors with lower k_{OH} while peroxide radicals ($[RO_2\cdot]$ and $[HO_2\cdot]$), which depend on both k_{OH} and $[\cdot OH]$, are similar for all precursors. This suggests that SOA mass yield is determined by precursor structure rather than gas-phase oxidation state since radical conditions for each aromatic hydrocarbon are comparable and $[RO_2\cdot]$ and $[HO_2\cdot]$ reactions are expected to determine SOA formation (Kroll and Seinfeld, 2008)

3.2 SOA chemical composition relationship with methyl group number

3.2.1 f_{44} vs f_{43}

Organic peaks at *m/z* 43 and *m/z* 44 are key fragments from AMS measurement toward characterization of oxygenated compounds in organic aerosol (Ng, et al., 2010;

Ng, et al., 2011). A higher f_{44} and a lower f_{43} indicates a higher degree of oxidation (Ng et al., 2010, 2011).The f_{44} and f_{43} evolution during SOA formation from different monocyclic aromatic hydrocarbon photooxidation is shown for low NO_x conditions (Fig. 2). Each marker type represents an individual monocyclic aromatic hydrocarbon with the marker colored by photooxidation time (light to dark). The f_{44} and f_{43} range are comparable to previous chamber studies with slight shift due to differences in initial conditions (e.g. NO_x etc.) (Ng, et al., 2010; Chhabra, et al., 2011; Loza, et al., 2012; Sato, et al., 2012). SOA compositions from monocyclic aromatic hydrocarbon photooxidation under low NO_x are in the LV-OOA and SV-OOA range of the f_{44} vs f_{43} triangle (Ng, et al., 2010) with those from benzene on the left side, toluene inside and other monocyclic aromatics on the right side of the triangle confirming that laboratory SOA f_{44} vs f_{43} is precursor dependent (Chhabra, et al., 2011). Evolution of SOA composition (Heald, et al., 2009; Jimenez, et al., 2009) refers to SOA chemical composition changes with time and f_{44} and f_{43} evolution refers to the change of f_{44} and f_{43} with time. Significant f_{44} and f_{43} evolution ~~trend~~ is observed for benzene and slightly for toluene ~~and~~, *m*-xylene and tetramethylbenzene.

Formatted: Subscript
Formatted: Subscript
Formatted: Subscript
Formatted: Subscript
Formatted: Subscript
Formatted: Subscript

In this work, average f_{44} and f_{43} are examined to demonstrate the methyl group impact on SOA chemical composition from monocyclic aromatic hydrocarbons. Average f_{44} vs f_{43} is marked with the aromatic compound name in Fig. 2. Generally decreasing f_{44} and increasing f_{43} are observed with increasing number of methyl groups on the aromatic ring. Similar trends are also observed in previous studies (Ng, et al., 2010; Chhabra et al., 2011; Sato, et al., 2012). The f_{44} vs f_{43} trend is quantified by linear curve fitting (f_{44}= -0.58 f_{43} + 0.19, R_2 = 0.94). f_{28} is assumed to be equal to f_{44} in the AMS frag Table of Unit Resolution Analysis, which describes the mathematical formulation of the apportionment at each unit resolution sticks to aerosol species, based on ambient studies (Zhang, et al., 2005; Takegawa et al., 2007) and CO^+/CO_2^+ ratio for SOA from aromatic oxidation is found around ~1 (0.9-1.3) (Chhabra et al., 2011). The slope of ~0.5 indicates that $2\Delta f_{44}=-\Delta f_{43}$ or $\Delta(f_{28}+f_{44}) =-\Delta f_{43}$ in SOA formed from monocyclic aromatic hydrocarbons with different numbers of methyl

groups. The CO_2^+ fragment ion at *m/z* 44 and $C_2H_3O^+$ fragment ion at *m/z* 43 are two major AMS fragmentation ions from aromatic secondary organic aerosol. No significant $C_3H_7^+$ is observed at *m/z* 43. CO_2^+ represents oxidized aerosol and is associated with carboxylic acids (Alfarra, et al., 2004, Aiken, et al., 2007, Takegawa, et al., 2007; Canagaratna, et al., 2015) while $C_2H_3O^+$ is associated with carbonyls (McLafferty and Turecek, 1993; Ng, et al., 2011). The CO^+ fragment ion at *m/z* 28 can originate from carboxylic acid or alcohol (Canagaratna, et al., 2015). The $\Delta(f_{28}+f_{44}) = -\Delta f_{43}$ relationship observed in this study imply that adding the methyl group to the aromatic ring changes SOA from CO_2^+ to $C_2H_3O^+$ implying a less oxidized SOA chemical composition in AMS mass fragments. While bicyclic hydrogen peroxides are considered to be the predominant species in aerosol phase from monocyclic aromatic photooxidation (Johnson, et al., 2004, 2005; Wyche, et al., 2009; Birdsall et al., 2010; Birdsall and Elrod, 2011; Nakao, et al., 2011), they are less likely to contribute to the CO_2^+ ion fragment. Possible mechanisms to produce SOA products that form the CO_2^+ fragments as well as produce $C_2H_3O^+$ fragments by adding methyl group are described in detail in Section 4.

3.2.2 H/C vs O/C

Elemental analysis (Aiken, et al., 2007, 2008) is used to elucidate SOA chemical composition and SOA formation mechanisms (Heald, et al., 2010; Chhabra, et al., 2011). Fig.3a shows the H/C and O/C time evolution of average SOA formed from hydrocarbon photooxidation of various monocyclic aromatics under low NO_x conditions (marked and colored similarly to Fig.2). The H/C and O/C ranges are comparable to previous chamber studies with slight shift due to difference in initial conditions (e.g. NO_x etc.) (Chhabra, et al., 2011; Loza, et al., 2012; Sato, et al., 2012). All data points are located in between slope=-1 and slope=-2 (Fig. 3a, lower left corner, zoom out panel). This suggests that SOA components from monocyclic aromatic photooxidation contain both carbonyl (ketone or aldehyde) and acid (carbonyl acid and hydroxycarbonyl) like functional groups. These elemental ratios

also confirm that SOA formed from monocyclic aromatic hydrocarbon photooxidation under low NO_x are among the LV-OOA and SV-OOA regions (Ng, et al., 2011). The change of elemental ratio (H/C and O/C) with time is referred as elemental ratio evolution. The elemental ratio evolution ~~trend~~ agrees with the f_{44} vs f_{43} ~~trend~~evolution (significant evolution in benzene and slightly for toluene, *m*-xylene and 1,2,4,5-tetramethylbenzene). This study concentrates on average H/C and O/C in order to demonstrate the methyl group impact on SOA chemical composition from monocyclic aromatic hydrocarbons.

Formatted: Font: Italic

Average H/C and O/C location is marked (Fig. 3a) for each aromatic compound by name. It is observed that H/C and O/C from SOA formed from *m*-xylene, 1, 2, 4-trimethylbenzene and monocyclic aromatics with more than three methyl groups are similarly distributed in H/C vs O/C. A general decrease in O/C and an increase in H/C are noted as the number of methyl groups on the aromatic ring increase, which is consistent with other studies (Chhabra, et al., 2011; Sato, et al., 2012). The trend indicates that monocyclic aromatics are less oxidized per carbon as the number of methyl groups increases, which can be attributed to less oxidation of the methyl groups compared to the aromatic ring carbons. The elemental ratio trends (O/C decreases and H/C increases as the number of methyl groups increases) are also consistent with the decreasing yield trends with increasing the number of methyl groups (Section 3.1), suggesting that SOA yield is dependent on SOA chemical composition. It should also be noticed that the higher O/C and lower H/C observed in SOA formed from 1,2,4-trimethylbenzne (three methyl substitute aromatic hydrocarbon) than that from *m*-xylene (two methyl substitute aromatic hydrocarbon) is due to the isomer impact on SOA chemical composition, which is discussed in details by Li, et al (2015). Further, the yield and O/C ratio agrees with recent findings that O/C ratio is well correlated to aerosol volatility (Section 3.3.2) (Cappa, et al., 2012, Yu, et al., 2014) thereby affecting the extent of gas to particle partitioning. The H/C vs O/C trend linear curve ($H/C = -1.34\ O/C + 2.00$, $R^2 = 0.95$) shows an approximately -1 slope with a y-axis (H/C) intercept of 2. The H/C vs O/C trend slope

Formatted: Font: Italic

observed in this work is similar to the toluene and *m*-xylene elemental ratio slope observed under high NO_x and H_2O_2 only conditions observed in Chhabra et al (2011).

The Van Krevelen diagram can also be used to analyze the oxidation pathway from initial SOA precursor to final SOA chemical composition by comparing the initial H/C and O/C ratios from the precursor hydrocarbon to the final SOA H/C and O/C ratios. Fig. 3b shows the aromatic precursor location on the left (texted with aromatic hydrocarbon name and colored by methyl group number) and average SOA chemical composition on the right. The SOA H/C increase in the final SOA chemical composition follows the initial aromatic precursor elemental ratio trend. A large O/C increase with a slight H/C increase is observed moving from precursor to SOA composition. SOA formation from hydroperoxide bicyclic compounds contributes to O/C increases without loss of H. The slight H/C increase might result from hydrolysis of ring opened product oligomerization (Jang and Kamens, 2001; Jang et al., 2002; Kalberer, et al., 2004; Sato, et al., 2012). A slight H/C decrease rather than increase is observed in the hexamethylbenzene data suggesting that the six methyl groups sterically inhibits certain reaction mechanism (eg. hydrolysis) to obtain H.

3.2.3 OS_c and its prediction

O/C alone may not capture oxidative changes as a result of breaking and forming of bonds (Kroll, et al., 2009). Oxidation state of carbon ($OS_c \approx 2O/C-H/C$) was introduced into aerosol phase component analysis by Kroll et al. (2011). It is considered to be a more accurate metric for describing oxidation in atmospheric organic aerosol (Ng et al., 2011; Canagaratna, et al., 2015; Lambe, et al., 2015) and therefore better correlated with gas-particle partitioning (Aumont, et al., 2012). Average SOA OS_c in this study ranges from -0.9 to 0.3 for monocyclic aromatic photooxidation under low NO_x conditions (Fig. 4b) and is comparable to previous studies (Kroll, et al., 2011 (toluene, *m*-xylene and trimethylbenzene); Sato, et al., 2012 (benzene and 1,3,5-trimethylbenzene)). OS_c observed is consistent with OS_c observed in field studies (Kroll, et al., 2011) especially in urban sites (e.g. -1.6～0.1, Mexico

City) and supports the major role of monocyclic aromatic precursors in producing anthropogenic aerosol. Average SOA OS_c values are consistent with the LV-OOA and SV-OOA regions (Ng, et al., 2011; Kroll, et al., 2011). OS_c only increases with oxidation time for benzene photooxidation (0.2～0.4).

The methyl group substitute ($-CH_3$) affects O/C and H/C ratios by increasing both carbon and hydrogen number as they relate to SOA OS_c. It is hypothesized here that the methyl group impacts remain similar in SOA elemental ratios as they do in the aromatic precursor ($-CH_3$ dilution effect). This would imply that the methyl group effect on SOA elemental ratio and OS_c from monocyclic aromatic hydrocarbons is predictable from benzene oxidation. Eq-1 and Eq-2 show the prediction formula for O/C and H/C, respectively, where *i* represents the methyl group number on the monocyclic aromatic precursor, $O/C_{benzene\_SOA}$ and $H/C_{benzene\_SOA}$ are the measured O/C and H/C in SOA from benzene photooxidation experiments.

$$O/C_{pre,i\_SOA} = \frac{6}{i+6}(O/C_{benzene\_SOA}) \quad \text{Eq-1}$$

$$H/C_{pre,i\_SOA} = \frac{2i}{i+6} + \frac{6}{i+6}(H/C_{benzene\_SOA}) \quad \text{Eq-2}$$

Fig. 4a shows a comparison of measured (red) and predicted (green) H/C and O/C location marked with corresponding SOA precursor methyl groups. The difference between predicted and measured H/C and O/C ranges from -6.4～1.2% and -11.8～20.9%, respectively. However, the predicted H/C vs O/C line (Eq-1 & Eq-2) is H/C= -1.38O/C +2.00. This is comparable to a measured data fitting line (Section 3.2.2 H/C= -1.34 O/C + 2.00, R_2 = 0.95). Predicted OS_c is then calculated based on the predicted H/C and O/C. Fig. 4b compares measured (red) and predicted (green) OS_c. The largest O/C and OS_c overestimation is observed in *m*-xylene (marked as 2 in Fig. 4a, bar 2 in Fig. 4b). This could be explained by the isomer selected for the two methyl group monocyclic aromatic hydrocarbon (*m*-xylene). A detailed analysis on isomer structure impact on SOA chemical composition is found in Li, et al (2015). The largest O/C and OS_c underestimation is observed in hexamethylbenzene (marked

as 6 in Fig. 4a, bar 6 in Fig. 4b). This suggests that the methyl groups attached to every aromatic carbon exert a steric inhibition effect on certain aromatic oxidation pathways, thus leading to increased importance of aerosol formation from other reaction pathways (possibly fragmentation Kroll, et al., 2011, see Section 4) to form SOA. It is also noticed that O/C and OS_c is slightly overestimated in SOA formed from pentamethylbenzene. This indicates that the methyl group hindrance impact on aromatic hydrocarbon oxidation should be explained by multiple pathways which have different impact on SOA formation.

Formatted: Subscript

The correlation between organic mass loading and chemical composition is also analyzed. Organic mass loading is well correlated (Pearson correlation~~R~~^{2}) with chemical composition parameters including f_{44} (0.907), f_{43} (-0.910), H/C (-0.890) and O/C (0.923) (Fig. S3). However, previous studies show that O/C and f_{44} decrease as organic mass loading increases (Shilling et al., 2009; Ng, et al., 2010; Pfaffenberger; 2013). The findings of this study indicate that molecular species drive SOA chemical composition rather than organic mass. The positive trend between f_{44} and organic mass loading is driven by benzene and toluene experiments (Fig. S3) where the high mass loading results are concurrent with high f_{44} results. However, the f_{44} change with mass loading increase during benzene and toluene photooxidation is less significant compared with the f_{44} difference caused by number of methyl groups on aromatic ring. Moreover, no significant correlation was found between mass loading and f_{44} or O/C when compared under similar mass loadings (including f_{44} at low mass loading time point of toluene and benzene photoxidation). Organic nitrate accounts for less than 10% organic in SOA components in all monocyclic aromatic hydrocarbon photooxidation experiments in this work according to AMS measurement and will not be discussed.

3.3 Physical property relationship with methyl group number

3.3.1 SOA Density

SOA mass density is a fundamental parameter in understanding aerosol morphology, dynamics, phase and oxidation (De Carol, et al., 2004; Katrib, et al., 2005; Dinar, et al., 2006; Cross, et al., 2007). SOA density ranged from 1.24-1.44 g/cm^3 for all aromatic-NO_x photooxidation experiments in this study. The range is comparable to previous studies under similar conditions (Ng, et al; 2007; Sato, et al., 2010; Esther Borrás, et al., 2012). A general decreasing density trend is found with increasing methyl group number on precursor aromatic rings (see Fig. 5a). Correlation between SOA density and chemical composition was statistically analyzed (Table S5). Besides the strong correlation with methyl group number (-0.943, Fig. 5a), SOA density was also well correlated with O/C ratio (0.873, Fig. 5b) and other measures of bulk chemical composition (Table S5). Bahreini et al (2005) reported a density increase trend with f_{44} in other compounds while Pang, et al. (2006) found that SOA density increases with O/C ratio. Kuwata, et al., 2011(Eq-3) and Nakao, et al., 2013 suggested a quantified relationship between SOA density and SOA elemental ratio. Eq-3 developed by

$$\rho = \frac{12+H/C+16\times O/C}{7+5\times H/C+4.15\times O/C} \qquad \text{Eq-3}$$

Kuwata, et al. (2011) is used in this work to predict density based on elemental ratio in order to explore the methyl group impact on SOA formation. Fig. 5c shows a good agreement between predicted and measured SOA densities (-6.58% ~ 10.42%). However, SOA density difference between prediction and measurement change from positive (0&1 methyl group) to negative (2,3,4 or 5 methyl groups) with increasing methyl group number~~SOA density underestimation enlarges with increasing methyl group number~~ (except hexamethylbenzene) implying that the increase of methyl groups promotes mechanism(s) leading to changes in the ratio of several key organic fragments (e.g., *m/z* 28 : *m/z* 44) thereby challenging the applicability of the default

fragment table for elemental ratio analysis. It is possible that CO^+/CO_2^+ and H_2O^+/CO_2^+ ratios are different in SOA formed from different aromatic precursors. Nakao, et al (2013) shows that H_2O^+/CO_2^+ increases with methyl group number due to the constant H_2O^+ fraction and a decrease in CO_2^+ fraction. Canagaratna, et al (2015) demonstrated that CO^+/CO_2^+ and H_2O^+/CO_2^+ are underestimated in certain compounds (especially alcohols). Assuming that the major impact of methyl group on SOA composition is to change –COOH to -$COCH_3$ (or other cyclic isomers), f_{CO2+} will decrease but H_2O^+ and CO^+ fraction might not change linearly. The alcohol contribution to CO^+/CO_2^+ and H_2O^+/CO_2^+ gradually grows as the methyl group prevents acid formation. Therefore, AMS measurements might underestimate O/C. This is consistent with the density prediction from elemental ratios where a change of error from positive to negative is seen as the number of methyl group change from less than two to two or more than two~~where a larger negative error is seen as the number of methyl groups increases~~, with the exception of hexamethylbenzene. This might relate to the difference in SOA formation pathways due to steric hindrance of the six methyl groups during hexamethylbenzene oxidation.

3.3.2 SOA Volatility

SOA volatility is a function of oxidation, fragmentation, oligomerization and SOA mass (Kalberer, et al., 2004; Salo, et al., 2011; Tritscher, et al., 2011; Yu, et al., 2014). Bulk SOA volatility can be described by the VFR after heating SOA to a fixed temperature in a thermodenuder. VFRs for SOA formed early in the experiment are around 0.2 for all monocyclic aromatic precursors and then increase as the experiment progresses. Increasing VFR indicates the gas to particle partitioning of more oxidized products, which may include oligomerization products formed during aromatic photooxidation. The VFR trends and ranges are comparable to previous studies (Kalberer et al., 2004; Qi et al., 2010a; Qi et al., 2010b; Nakao et al., 2012). Fig. 6a shows the relationship between SOA precursor methyl group number and SOA VFR at the end of the experiment (VFR_{end}). VFR shows a significant decreasing trend with

increasing methyl group number from benzene to 1, 2, 4, 5-tetramethylbenzene. This implies that volatility of SOA-forming products increases as the number of methyl groups on the aromatic ring increases. There is also a slight increase in VFR from 1, 2, 4, 5-tetramethylbenzene to hexamethylbenzene; however, VFR in SOA formed from all C_{10+} group aromatics is lower than that of 1, 2, 4-trimethylbenzene. The changing VFR trend suggests that chemical components contributing to SOA formation become different when more than four methyl groups are attached to a single aromatic ring. A positive correlation (0.755, p=0.05) found between mass loading and VFR_{end} implies that the lower the volatility in the products formed from aromatic hydrocarbons, the higher the SOA mass concentration. An opposite correlation between mass loading and VFR is found in previous studies due to the partitioning of more volatile compounds to the particle phase at high mass loading (Tritscher, et al., 2011;Salo, et al., 2011). Therefore, mass loading does not directly lead to the VFR trend in the current study, rather it is the methyl group number in the SOA precursor that affects the composition of SOA and therefore the monocyclic aromatic hydrocarbon yield (section 3.1) and volatility. The correlation between SOA volatility (VFR) and chemical composition is statistically analyzed (Table S5). O/C (0.937, p = 0.002) and OS_c (0.932, p = 0.02)~~O/C (0.932, p=0.02) and OS_c (0.931, p=0.02)~~ have the highest correlation with VFR_{end}. Previous studies also observed that lower aerosol volatility is correlated to higher O/C ratio (Cappa, et al., 2012, Yu, et al., 2014) and OS_c (Aumont, et al., 2012; Hildebrandt Ruiz, et al., 2014). Fig. 6b and Fig. 6c illustrate the VFR_{end} and O/C or OS_c relationship among all the monocyclic aromatic precursors investigated in this study. Benzene and toluene are located on the right upper corner in both graphs suggesting that significantly more oxidized and less volatile components are formed from monocyclic aromatic precursors with less than two methyl groups. The VFR_{end} and chemical components relationship becomes less significant when only monocyclic aromatic precursors with more than two methyl groups are considered.

Formatted: Subscript

4. Discussion

4. 1 SOA formation pathway from monocyclic aromatic hydrocarbon

Bicyclic peroxide compounds are considered to be important SOA forming products from monocyclic aromatic photooxidation (Johnson, et al., 2004, 2005; Song, et al., 2005; Wyche, et al., 2009; Birdsall et al., 2010; Birdsall and Elrod, 2011; Nakao, et al., 2011). However, the significant CO_2^+ fragment (f_{44}) observed for SOA by the AMS indicates a contribution of an additional pathway to SOA formation from monocyclic aromatic hydrocarbon photooxidation since it is unlikely that bicyclic peroxides could produce a CO_2^+ in the AMS. Hydrogen abstraction from the methyl group is not further discussed here as it accounts for less than 10% monocyclic aromatic oxidation pathway (Calvert, et al., 2002). However, it is important to consider the further reaction of bicyclic peroxide ring scission products, especially in the presence of NO_x (Jang and Kamens, 2001; Atkinson and Arey, 2003; Song, et al., 2005; Hu, et al., 2007; Birdsall and Elrod, 2011; Carter, et al., 2013). First generation ring scission products include 1, 2-dicarbonyls (glyoxal and methylglyoxal) and unsaturated 1, 4-dicarbonyls (Forstner, et al., 1997; Jang and Kamens, 2001; Birdsall and Elrod, 2011). These dicarbonyls are small volatile molecules that are unlikely to directly partition into the particle phase. However, these small molecules can potentially to grow into low volatility compounds through oligomerization. Previous studies suggest that oligomerization can be an important pathway for SOA formation from monocyclic aromatic precursors (Edney, et al., 2001; Baltensperger, et al., 2005; Hu, et al., 2007; Sato, et al., 2012). While Kalberer, et al (2004) proposed an oligomerization pathway of 1, 2-dicarbonyls, Arey, et al (2008) found that unsaturated 1, 4-dicarbonyls have a higher molar yield than 1, 2-dicarbonyls in OH radical-initiated reaction of monocyclic aromatic hydrocarbons. Further, OH radical reaction and photolysis rates are observed to be lower in 1, 2-dicarbonyls photolysis (Plum, et al., 1983; Chen, et al., 2000; Salter, et al., 2013; Lockhart, et al; 2013) than unsaturated 1, 4-dicarbonyls (Bierbach, et al., 1994; Xiang, et al; 2007). This suggests

that secondary reaction of unsaturated 1, 4-dicarbonyls is more important than that of 1, 2-dicarbonyls. Previous studies have found that unsaturated 1, 4-dicarbonyls react to form small cyclic furanone compounds (Jang, et al., 2001; Bloss, et al., 2005; Aschmann, et al., 2011). Oligomerization is possible for these small cyclic compounds based on their similar molecular structure with glyoxal and methylglyoxal (Fig. 7 c-2-1 & c-2-2 pathway, Fig. S4). Products from further oligomerization of ring opening compounds can also partition into the aerosol phase and contribute to SOA formation. Hydrolysis is necessary in both oligomerization pathways (Fig. S4 and Kalberer, et al., 2004), which is consistent with the slight H/C increase observed for most monocyclic aromatic hydrocarbon photooxidation results in this study. However, Nakao et al. (2012) showed that the glyoxal impact on SOA formation is majorly due to OH radical enhancement with glyoxal instead of oligomerization, especially under dry conditions. This indicates that oligomerization from small cyclic furanone is more likely to contribute more to SOA formation than 1, 2- dicarbonyl in this work. Other pathways reported in previous studies are also possible to contribute to SOA formation here (Edney, et al., 2001 (polyketone); Jang and Kamens, 2001 (aromatic ring retaining products; six and five member non-aromatic ring products; ring opening products); Bloss, et al., 2005 (benzoquinone, epoxide, phenol); Carter, 2013 (bicyclic hydroperoxide)). Our work only addresses differences in the oligomerization pathway contribution to form SOA from monocyclic aromatic hydrocarbons.

A simplified monocyclic aromatic oxidation mechanism for low NO_x conditions is shown (Fig. 7 & Fig. 8; the figures only illustrate monocyclic aromatic oxidation related to particle formation). Fig. 7 illustrates the oxidation, fragmentation and oligomerization after initial OH addition to aromatic ring, Fig. 8 shows the kinetic scheme for SOA formation from monocyclic aromatic hydrocarbons. S_1, S_2 and S_3 represent bicyclic hydroperoxide compounds, ring opening compounds and oligomerization products, respectively. Table S6 summarizes the predicted vapor pressures of the benzene photooxidation products using SIMPOL (Pankow and Asher, 2008). The bicyclic hydroperoxide (S_1, Fig. 8) is more volatile than the oligomers (S_3

in Fig. 8). The volatilities of the bicyclic hydroperoxides are sufficiently high to allow additional oxidation (e.g. add one more hydroperoxide functional group to form $C_6H_6O_8$). The further oxidized bicyclic hydroperoxide vapor pressure is predicted to be similar to oligomerization products from reaction of c-2-1 (Fig. S4) with glyoxal. The higher vapor pressure of oligomer products from glyoxal as compared to oligomers from other products indicates that bicyclic hydroperoxides (S_1) contribute more to SOA formation in benzene than oligomerization products (~~S_2~~S_3), especially at higher particle mass loadings, as compared with monocyclic aromatic hydrocarbons containing methyl groups according to the two product model fitting (Fig. 1 and Table. 2).

4. 2 Methyl group number impact on SOA formation pathway from monocyclic aromatic hydrocarbon

It is observed that as the number of methyl groups on the monocyclic aromatic precursor increases, mass yield (Section 3.1), overall oxidation per carbon (Section 3.2), and SOA density all decrease and SOA volatility increases. The observed yield trend is attributed to the increasing methyl group number enhancing aromatic fragmentation and inhibiting oligomerization. First, the methyl group stabilizes the ring opening radical (Atkinson, 2007; Ziemann, 2011), thus favoring the ring opening pathway. Second, the methyl group hinders cyclic compound formation and oligomerization (Fig. 7). Oligomerization is unlikely to occur directly from non-cyclic dicarbonyls (Kalberer, et al, 2004) or indirectly from cyclic compounds formed by unsaturated dicarbonyls (Fig. S5) with increasing methyl group number. Methyl groups both inhibit oligomerization (Fig.7 (c-1-3)) and prevent the formation of cyclic compounds from unsaturated dicarbonyls (Fig.7 (c-2-3)) when methyl groups are attached to both ends of an unsaturated dicarbonyl. Oligomerization is possible for these ketones through reactions such as aldol condensation and hemiacetal formation (Jang et al., 2002) under acidic conditions. However, this is less favored for the current study in the absence of acidic seeds. Hence, less cyclic compounds are

available for subsequent oligomerization, leading to more volatile products and a decrease in SOA formation. Moreover, the SOA composition trend is well explained by a $-CH_3$ dilution effect. Previous studies on the different gas phase (Forstner, et al., 1997; Yu, et al., 1997) and particle phase (Hamilton, et al., 2005; Sato, et al., 2007; Sato, et al., 2012) products supports this methyl group dilution theory. A typical example is that more 3-methyl-2,5-furandione is observed in *m*-xylene than toluene and vice versa for 2,5-furandione. Sato et al. (2010) suggests that more low-reactive ketones are produced rather than aldehydes with increasing number of substituents. However, most ketones or aldehydes detected are so volatile that they mostly exist in the gas phase (Forstner, et al., 1997; Yu, et al., 1997; Cocker, et al., 2001b; Jang and Kamens, 2001). Taken collectively, this implies the importance of oligomerization and methyl substitutes on SOA formation.

The observation of a slight H/C decrease from hexamethylbenzene to its SOA components in contrast with the increasing trend for monocyclic aromatic photooxidation for zero to five methyl group substitutes (Section 3.2.2) suggests that hydrolysis followed by oligomerization might not be significant when all aromatic ring carbons have attached methyl groups. Besides, the higher O/C and lower H/C (or the higher OS_c) than predicted in Section 3.2.3 indicates that SOA components from hexamethylbenzene photooxidation are more oxidized per carbon due to oxidation of the methyl groups, which is possibly related to the steric hindrance of the six methyl groups. Moreover, there is a slightly increasing trend in VFR from 1, 2, 4, 5-tetramethylbenzene to hexamethylbenzene (Section 3.3.2). Further studies (e.g. photooxidation using isotope labeled methyl group hexamethylbenzene) are required to probe the unique SOA aspects from hexamethylbenzene photooxidation.

5. Atmospheric Implication

The impact of the number of methyl group substituents on SOA formation has been comprehensively studied in this work by integrating SOA yield with SOA chemical composition and SOA physical properties. A generally decreasing trend is found in

the SOA mass yield and the carbon number averaged oxidation level with increasing number of methyl groups. SOA physical properties agree with yield and oxidation results. Therefore, this study demonstrates that the addition of methyl group substitutes to monocyclic aromatic precursors decreases the oxidation of aromatic hydrocarbon to less volatile compounds~~aromatic aging~~. Offsetting the amount of CO_2^+ and $C_2H_3O^+$ suggests a methyl group dilution effect on SOA formation from monocyclic aromatic hydrocarbons. The proposed methyl group dilution effect is then applied successfully to the predict SOA elemental ratio. Overall, this study clearly demonstrates the methyl group impact on SOA formation from monocyclic aromatic hydrocarbons.

Benzene and toluene are evaluated as the most important monocyclic aromatic precursors to SOA formation among the six compounds studied due to their high SOA yields and highly oxidized components. Hexamethylbenzene is found to be significantly more oxidized than predicted based on other monocyclic aromatic hydrocarbons studied here. This implies uniqueness in the methyl group behavior (no –H on aromatic ring) in hexamethylbenzene. Oligomerization is proposed to be an important pathway for SOA formation from monocyclic aromatic hydrocarbons. It is likely that oligomerization is even more valuable to SOA formation from monocyclic aromatic hydrocarbons under polluted areas (catalyzed effect, Jang, et al., 2002; Iinuma, et al., 2004; Noziere, et al., 2008) and ambient humidity (Liggio, et al., 2005a, b; Hastings, et al., 2005).

Acknowledgements

We acknowledge funding support from National Science Foundation (ATM 0901282) and W. M. Keck Foundation. Any opinions, findings, and conclusions expressed in this material are those of the author(s) and do not necessarily reflect the views of the NSF.

References

Aiken, A. C., DeCarlo, P. F. and Jimenez, J. L.: Elemental analysis of organic species with electron ionization high-resolution mass spectrometry, Anal. Chem., 79(21), 8350-8358, doi:10.1021/ac071150w, 2007.

Aiken, A. C., DeCarlo, P. F., Kroll, J. H., Worsnop, D. R., Huffman, J. A., Docherty, K. S., Ulbrich, I. M., Mohr, C., Kimmel, J. R., Sueper, D., Sun, Y., Zhang, Q., Trimborn, A., Northway, M., Ziemann, P. J., Canagaratna, M. R., Onasch, T. B., Alfarra, M. R., Prevot, A. S. H., Dommen, J., Duplissy, J., Metzger, A., Baltensperger, U. and Jimenez, J. H.: O/C and OM/OC ratios of primary, secondary, and ambient organic aerosols with high-resolution time-of-flight aerosol mass spectrometry, Environ. Sci. Technol., 42(12), 4478-4485, doi:10.1021/es703009q, 2008.

Alfarra, M. R., Coe, H., Allan, J. D., Bower, K. N., Boudries, H., Canagaratna, M. R., Jimenez, J. L., Jayne, J. T., Garforth, A. A., Li, S-M. and Worsnop, D. R.: Characterization of urban and rural organic particulate in the lower Fraser valley using two aerodyne aerosol mass spectrometers, Atmos. Environ., 38(34), 5745-5758, doi:10.1016/j.atmosenv.2004.01.054, 2004.

Arey, J., Obermeyer, G., Aschmann, S. M., Chattopadhyay, S., Cusick, R. D. and Atkinson, R.: Dicarbonyl products of the OH radical-initiated reaction of a series of aromatic hydrocarbons, Environ. Sci. Technol., 43(3), 683-689, doi:10.1021/es8019098, 2008.

Aschmann, S. M., Arey, J. and Atkinson, R.: Rate constants for the reactions of OH radicals with 1, 2, 4, 5-tetramethylbenzene, pentamethylbenzene, 2, 4, 5-trimethylbenzaldehyde, 2, 4, 5-trimethylphenol, and 3-methyl-3-hexene-2, 5-dione and products of OH+ 1, 2, 4, 5-tetramethylbenzene, J. Phys. Chem. A., 117(12), 2556-2568, doi:10.1021/jp400323n, 2013.

Aschmann, S. M., Nishino, N., Arey, J. and Atkinson, R.: Kinetics of the Reactions of OH Radicals with 2-and 3-Methylfuran, 2, 3-and 2, 5-Dimethylfuran, and E-and Z-3-Hexene-2, 5-dione, and Products of OH+ 2, 5-Dimethylfuran, Environ. Sci. Technol., 45(5), 1859-1865., doi:10.1021/es103207k, 2011.

Atkinson, R.: Rate constants for the atmospheric reactions of alkoxy radicals: An updated estimation method, Atmos. Environ., 41(38), 8468-8485, doi:10.1016/j.atmosenv.2007.07.002, 2007.

Atkinson, R. and Arey, J.: Atmospheric degradation of volatile organic compounds, Chem. Rev., 103(12), 4605-4638, doi:10.1021/cr0206420, 2003.

Aumont, B., Valorso, R., Mouchel-Vallon, C., Camredon, M., Lee-Taylor, J. and Madronich, S.: Modeling SOA formation from the oxidation of intermediate volatility n-alkanes, Atmos. Chem. Phys., 12(16), 7577-7589, doi:10.5194/acp-12-7577-2012, 2012.

Bahreini, R., Keywood, M. D., Ng, N. L., Varutbangkul, V., Gao, S., Flagan, R. C., Seinfeld, J. H., Worsnop, D. R. and Jimenez, J. L.: Measurements of secondary organic aerosol from oxidation of cycloalkenes, terpenes, and *m*-xylene using an Aerodyne aerosol mass spectrometer, Environ. Sci. Technol., 39(15), 5674-5688, doi:10.1021/es048061a, 2005.

Baltensperger, U., Kalberer, M., Dommen, J., Paulsen, D., Alfarra, M. R., Coe, H., Fisseha, R., Gascho, A., Gysel, M., Nyeki, S., Sax, M., Steinbacher, M., Prevot, A. S. H., Sjögren, S., Weingartnera, E. and Zenobib, R.: Secondary organic aerosols from anthropogenic and biogenic precursors, Faraday. Discuss, 130, 265-278, doi:10.1039/b417367h, 2005.

Bierbach, A., Barnes, I., Becker, K. H. and Wiesen, E.: Atmospheric chemistry of unsaturated carbonyls: Butenedial, 4-oxo-2-pentenal, 3-hexene-2, 5-dione, maleic anhydride, 3H-furan-2-one, and 5-methyl-3H-furan-2-one, Environ. Sci. Technol, 28(4), 715-729, doi:10.1021/es00053a028, 1994.

Birdsall, A. W., Andreoni, J. F. and Elrod, M. J.: Investigation of the role of bicyclic peroxy radicals in the oxidation mechanism of toluene, J. Phys. Chem. A., 114(39), 10655-10663, doi:10.1021/jp105467e, 2010.

Birdsall, A. W. and Elrod, M. J.: Comprehensive NO-dependent study of the products of the oxidation of atmospherically relevant aromatic compounds, J. Phys. Chem. A., 115(21), 5397-5407, doi:10.1021/jp2010327, 2011.

Bloss, C., Wagner, V., Jenkin, M. E., Volkamer, R., Bloss, W. J., Lee, J. D., Heard, D. E., Wirtz, K., Martin-Reviejo, M., Rea, G, Wenger, J. C., and Pilling M. J.: Development of a detailed chemical mechanism (MCMv3. 1) for the atmospheric oxidation of aromatic hydrocarbons, Atmos. Chem. Phys., 5(3), 641-664, doi:10.5194/acp-5-641-2005, 2005.

Borrás, E. and Tortajada-Genaro, L. A.: Secondary organic aerosol formation from the photo-oxidation of benzene, Atmos. Environ., 47, 154-163, doi:10.1016/j.atmosenv.2011.11.020, 2012.

Buczynska, A. J., Krata, A., Stranger, M., Godoi, A. F. L., Kontozova-Deutsch, V., Bencs, L., Naveau, I., Roekens, E. and Van Grieken, R.: Atmospheric BTEX-concentrations in an area with intensive street traffic, Atmos. Environ., 43(2), 311-318, doi:10.1016/j.atmosenv.2008.09.071, 2009.

Calvert, J. G., Atkinson, R., Becker, K. H., Kamens, R. M., Seinfeld, J. H., Wallington, T. J. and Yarwood, G.: The mechanisms of atmospheric oxidation of aromatic hydrocarbons, Oxford University Press New York, 2002.

Canagaratna, M. R., Jayne, J. T., Jimenez, J. L., Allan, J. D., Alfarra, M. R., Zhang, Q., Onasch, T. B., Drewnick, F., Coe, H., Middlebrook, A., Delia, A., Williams, L. R., Trimborn, A. M., Northway, M. J., DeCarlo, P. F., Kolb, C. E., Davidovits, P. and Worsnop D. R.: Chemical and microphysical characterization of ambient aerosols with the aerodyne aerosol mass spectrometer, Mass. Spectrom. Rev., 26(2), 185-222, doi:10.1002/mas.20115, 2007.

Canagaratna, M. R., Jimenez, J. L., Kroll, J. H., Chen, Q., Kessler, S. H., Massoli, P., Hildebrandt Ruiz, L., Fortner, E., Williams, L. R., Wilson, K. R., Surratt, J. D., Donahue, N. M., Jayne, J. T. and Worsnop, D. R.: Elemental ratio measurements of organic compounds using aerosol mass spectrometry: characterization, improved calibration, and implications, Atmos. Chem. Phys., 15(1), 253-272, doi:10.5194/acp-15-253-2015, 2015.

Cappa, C. D. and Wilson, K. R.: Multi-generation gas-phase oxidation, equilibrium partitioning, and the formation and evolution of secondary organic aerosol, Atmos. Chem. Phys., 12(20), 9505-9528, doi:10.5194/acp-12-9505-2012, 2012.

Carter, W. P. L. and Heo, G.: Development of revised SAPRC aromatics mechanisms, Atmos. Environ., 77, 404-414, doi:10.1016/j.atmosenv.2013.05.021, 2013.

Carter, W. P. L., Cocker III, D. R., Fitz, D. R., Malkina, I.L., Bumiller, K., Sauer, C.G., Pisano, J.T., Bufalino, C., Song, C.: A new environmental chamber for evaluation of gas-phase chemical mechanisms and secondary aerosol formation, Atmos. Environ., 39(40), 7768-7788, doi:10.1016/j.atmosenv.2005.08.040, 2005.

–Carter, W. P. L. and Heo, G.: Development of Revised SAPRC Aromatics Mechanisms, California Air Resources Board, Sacramento, CA, USA, 2012.Chan, A. W. H., Kroll, J. H., Ng, N. L. and Seinfeld, J. H.: Kinetic modeling of secondary organic aerosol formation: effects of particle-and gas-phase reactions of semivolatile products, Atmos. Chem. Phys., 7(15), 4135-4147, doi:10.5194/acp-7-4135-2007,2007.

Chen, Y., Wang, W. and Zhu, L.: Wavelength-dependent photolysis of methylglyoxal in the 290-440 nm region, J. Phys. Chem. A., 104(47), 11126-11131, doi:10.1021/jp002262t, 2000.

Chhabra, P. S., Ng, N. L., Canagaratna, M. R., Corrigan, A. L., Russell, L. M., Worsnop, D. R., Flagan, R. C. and Seinfeld, J. H.: Elemental composition and oxidation of chamber organic aerosol, Atmos. Chem. Phys., 11(17), 8827-8845, doi:10.5194/acp-11-8827-2011, 2011.

Cocker III, D. R.., Flagan, R. C. and Seinfeld, J. H.: State-of-the-art chamber facility for studying atmospheric aerosol chemistry, Environ. Sci. Technol., 35(12), 2594-2601, doi:10.1021/es0019169, 2001.

Cocker III, D. R., Mader, B. T., Kalberer, M., Flagan, R.C. and Seinfeld, J. H.: The effect of water on gas–particle partitioning of secondary organic aerosol: II. *m*-xylene and 1, 3, 5-trimethylbenzene photooxidation systems, Atmos. Environ., 35(35), 6073-6085, doi:10.1016/S1352-2310(01)00405-8, 2001.

Cross, E. S., Slowik, J. G., Davidovits, P., Allan, J. D., Worsnop, D. R., Jayne, J. T., Lewis, D. K., Canagaratna, M. and Onasch, T. B.: Laboratory and ambient particle density determinations using light scattering in conjunction with aerosol mass spectrometry, Aerosol Sci. Tech., 41(4), 343-359., doi:10.1080/02786820701199736, 2007.

Darouich, T. Al., Behar, F. and Largeau., C.: Thermal cracking of the light aromatic fraction of Safaniya crude oil–experimental study and compositional modelling of molecular classes. Org. Geochem., 37(9), 1130-1154, doi:. 10.1016/j.orggeochem.2006.04.003, 2006

DeCarlo, P. F., Kimmel, J. R., Trimborn, A., Northway, M. J., Jayne, J. T., Aiken, A. C., Gonin, M., Fuhrer, K., Horvath, T., Docherty, K. S., Worsnop, D. R. and Jimenez, J. L.: Field-deployable, high-resolution, time-of-flight aerosol mass spectrometer. Anal. Chem., 78(24), 8281-8289, doi:10.1021/ac061249n, 2006.

DeCarlo, P. F., Slowik, J. G., Worsnop, D. R., Davidovits, P. and Jimenez, J. L.: Particle morphology and density characterization by combined mobility and aerodynamic diameter measurements. Part 1: Theory, Aerosol Sci. Tech., 38(12), 1185-1205, doi:10.1080/027868290903907, 2004.

Diehl, J. W. and Sanzo, F. P. Di.: Determination of aromatic hydrocarbons in gasolines by flow modulated comprehensive two-dimensional gas chromatography, J. Chromatogr. A., 1080(2): 157-165, doi:10.1016/j.chroma.2004.11.054, 2005.

Dinar, E., Mentel, T. and Rudich, Y.: The density of humic acids and humic like substances (HULIS) from fresh and aged wood burning and pollution aerosol particles, Atmos. Chem. Phys., 6(12), 5213-5224, doi:10.5194/acp-6-5213-2006, 2006.

Duplissy, J., DeCarlo, P. F., Dommen, J., Alfarra, M. R., Metzger, A., Barmpadimos, I., Prevot, A. S., Weingartner, E., Tritscher, T. and Gysel, M.: Relating hygroscopicity and composition of organic aerosol particulate matter, Atmos. Chem. Phys., 11(3), 1155-1165, doi:10.5194/acp-11-1155-2011, 2011.

Edney, E., Driscoll, D., Weathers, W., Kleindienst, T., Conver, T., McIver, C. and Li, W.: Formation of polyketones in irradiated toluene/propylene/NO_x/air mixtures, Aerosol Science & Technology, 35(6), 998-1008, doi:10.1080/027868201753306769, 2001.

Forstner, H. J. L., Flagan, R. C. and Seinfeld, J. H.: Secondary organic aerosol from the photooxidation of aromatic hydrocarbons: Molecular composition, Environ. Sci. Technol., 31(5), 1345-1358, doi:10.1021/es9605376, 1997.

Fraser, M. P., Cass, G. R., Simoneit, B. R. and Rasmussen, R.: Air quality model evaluation data for organics. 5. C_6-C_{22} nonpolar and semipolar aromatic compounds, Environ. Sci. Technol., 32(12), 1760-1770, doi:10.1021/es970349v, 1998.

Glasson, W. A. and Tuesday, C. S.: Hydrocarbon reactivities in the atmospheric photooxidation of nitric oxide, Environ. Sci. Technol., 4(11), 916-924., doi:10.1021/es60046a002, 1970.

Hallquist, M., Wenger, J. C., Baltensperger, U., Rudich, Y., Simpson, D., Claeys, M., Dommen, J., Donahue, N. M., George, C., Goldstein, A. H., Hamilton, J. F., Herrmann, H., Hoffmann, T., Iinuma, Y., Jang, M., Jenkin, M. E., Jimenez, J. L., Kiendler-Scharr, A., Maenhaut, W., McFiggans, G., Mentel, Th. F., Monod, A., Prévôt, A. S. H., Seinfeld, J. H., Surratt, J. D., Szmigielski, R. and Wildt, J.: The formation, properties and impact of secondary organic aerosol: current and emerging issues, Atmos. Chem. Phys., 9(14), 5155-5236, doi:10.5194/acp-9-5155-2009, 2009.

Hamilton, J. F., Webb, P. J., Lewis, A. C. and Reviejo, M. M.: Quantifying small molecules in secondary organic aerosol formed during the photo-oxidation of toluene with hydroxyl radicals, Atmos. Environ., 39(38), 7263-7275, doi:10.1016/j.atmosenv.2005.09.006, 2005.

Hastings, W. P., Koehler, C. A., Bailey, E. L. and De Haan, D. O.: Secondary organic aerosol formation by glyoxal hydration and oligomer formation: Humidity effects and

equilibrium shifts during analysis, Environ. Sci. Technol., 39(22), 8728-8735, doi:10.1021/es050446l, 2005.

Heald, C. L., Kroll, J. H., Jimenez, J. L., Docherty, K. S., DeCarlo, P. F., Aiken, A. C., Chen, Q., Martin, S. T., Farmer, D. K. and Artaxo, P.: A simplified description of the evolution of organic aerosol composition in the atmosphere, Geophys. Res. Lett, 37(8), L08803, doi:10.1029/2010GL042737, 2010.

Henze, D. K., Seinfeld, J. H., Ng, N. L., Kroll, J. H., Fu, T-M., Jacob, D. J., Heald, C. L.: Global modeling of secondary organic aerosol formation from aromatic hydrocarbons: high-vs. low-yield pathways, Atmos. Chem. Phys., 8(9), 2405-2421, doi:10.5194/acp-8-2405-2008, 2008.

Hildebrandt Ruiz, L., Paciga, A., Cerully, K., Nenes, A., Donahue, N. M. and Pandis, S. N.: Aging of secondary organic aerosol from small aromatic VOCs: changes in chemical composition, mass yield, volatility and hygroscopicity, Atmos. Chem. Phys. Disc., 14(22), 31441-31481, doi:10.5194/acpd-14-31441-2014, 2014.

Holzinger, R., Kleiss, B., Donoso, L. and Sanhueza, E.: Aromatic hydrocarbons at urban, sub-urban, rural (8° 52′ N; 67° 19′ W) and remote sites in Venezuela, Atmos. Environ., 35(29), 4917-4927, doi:10.1016/S1352-2310(01)00286-2, 2001.

Hu, D. and Kamens, R. M.: Evaluation of the UNC toluene-SOA mechanism with respect to other chamber studies and key model parameters, Atmos. Environ., 41(31), 6465-6477, doi:10.1016/j.atmosenv.2007.04.026, 2007.

Hu, D., Tolocka, M., Li, Q. and Kamens, R. M.: A kinetic mechanism for predicting secondary organic aerosol formation from toluene oxidation in the presence of NOx and natural sunlight, Atmos. Environ., 41(31), 6478-6496, doi:10.1016/j.atmosenv.2007.04.025, 2007.

Hu, L., Millet, D. B., Baasandorj, M., Griffis, T. J., Travis, K. R., Tessum, C. W., Marshall, J. D., Reinhart, W. F., Mikoviny, T., Müller, M., Wisthaler, A., Graus, M., Warneke, C., and de Gouw, J.:Emissions of C_6–C_8 aromatic compounds in the United States: Constraints from tall tower and aircraft measurements, J. Geophys. Res.-Atmos., 120(2), 826-842, doi:10.1002/2014JD022627, 2015.

Iinuma, Y., Böge, O., Gnauk, T. and Herrmann, H.: Aerosol-chamber study of the α-pinene/O_3 reaction: influence of particle acidity on aerosol yields and products, Atmos. Environ., 38(5), 761-773, doi:10.1016/j.atmosenv.2003.10.015, 2004.

Jang, M., Czoschke, N. M., Lee, S., and Kamens, R. M.: Heterogeneous atmospheric aerosol production by acid-catalyzed particle-phase reactions, Science, 298(5594), 814-817, doi:10.1126/science.1075798, 2002.

Jang, M. and Kamens, R.M.: Characterization of secondary aerosol from the photooxidation of toluene in the presence of NO_x and 1-propene, Environ. Sci. Technol., 35(18), 3626-3639, doi:10.1021/es010676+, 2001.

Jimenez, J. L., Canagaratna, M. R., Donahue, N. M., Prevot, A. S. H., Zhang, Q., Kroll, J. H., DeCarlo, P. F., Allan, J. D., Coe, H., Ng, N. L., Aiken, A. C., Docherty, K. S., Ulbrich, I. M., Grieshop, A. P., Robinson, A. L., Duplissy, J., Smith, J. D., Wilson, K. R., Lanz, V. A., Hueglin, C., Sun, Y. L., Tian, J., Laaksonen, A., Raatikainen, T., Rautiainen, J., Vaattovaara, P., Ehn, M., Kulmala, M., Tomlinson, J. M., Collins, D. R., Cubison, M. J., Dunlea1, E., J., Huffman, J. A., Onasch, T. B., Alfarra, M. R., Williams, P. I., Bower, K., Kondo, Y., Schneider, J., Drewnick, F., Borrmann, S., Weimer, S.,, Demerjian, K., Salcedo, D., Cottrell, L., Griffin, R., Takami, A., Miyoshi, T., Hatakeyama, S., Shimono, A., Sun, J. Y., Zhang, Y. M., Dzepina, K., Kimmel, J. R., Sueper, D., J. Jayne, T., Herndon, S. C., Trimborn, A. M., Williams, L. R., Wood, E. C., Middlebrook, A. M., Kolb C. E., Baltensperger, U. and Worsnop D. R.: Evolution of organic aerosols in the atmosphere, Science, 326(5959), 1525-1529, doi:10.1126/science.1180353, 2009.

Johnson, D., Jenkin, M. E., Wirtz, K., Martin-Reviejo, M.: Simulating the formation of secondary organic aerosol from the photooxidation of aromatic hydrocarbons, Environ. Chem., 2(1), 35-48, doi:10.1071/EN04079, 2005.

Johnson, D., Jenkin, M. E., Wirtz, K., Martin-Reviejo, M.: Simulating the formation of secondary organic aerosol from the photooxidation of toluene, Environ. Chem., 1(3), 150-165, doi:10.1071/EN04069, 2004.

Kalberer, M., Paulsen, D., Sax, M., Steinbacher, M., Dommen, J., Prevot, A. S. H., Fisseha, R., Weingartner, E., Frankevich, V. and Zenobi, R.: Identification of polymers as major components of atmospheric organic aerosols, Science, 303(5664), 1659-1662, doi:10.1126/science.1092185, 2004.

Kanakidou, M., Seinfeld, J. H., Pandis, S. N., Barnes, I., Dentener, F. J, Facchini, M. C., Van Dingenen, R., Ervens, B., Nenes, A., Nielsen, C. J., Swietlicki, E., Putaud, J. P., Balkanski, Y., Fuzzi, S., Horth, J., Moortgat, G. K., Winterhalter, R., Myhre, C. E. L., Tsigaridis, K., Vignati, E., Stephanou, E. G., and Wilson, J.: Organic aerosol and global climate modelling: a review, Atmos. Chem. Phys., 5(4), 1053-1123, doi:10.5194/acp-5-1053-2005, 2005.

Katrib, Y., Martin, S. T., Rudich, Y., Davidovits, P., Jayne, J. T. and Worsnop, D. R.: Density changes of aerosol particles as a result of chemical reaction, Atmos. Chem. Phys., 5(1), 275-291, doi:10.5194/acp-5-275-2005, 2005.

Kleindienst, T. E., Smith, D. F., Li, W., Edney, E. O., Driscoll, D. J., Speer, R. E. and Weathers, W. S.: Secondary organic aerosol formation from the oxidation of aromatic hydrocarbons in the presence of dry submicron ammonium sulfate aerosol, Atmos. Environ., 33(22), 3669-3681, doi:10.1016/S1352-2310(99)00121-1, 1999.

Kroll, J. H., Donahue, N. M., Jimenez, J. L., Kessler, S. H., Canagaratna, M. R., Wilson, K. R., Altieri, K .E., Mazzoleni, L. R., Wozniak, A. S., Bluhm, H., Mysak, E. R., Smith, J. D., Kolb, C. E. and Worsnop D. R.: Carbon oxidation state as a metric for describing the chemistry of atmospheric organic aerosol, Nature Chemistry, 3(2), 133-139, doi:10.1038/nchem.948, 2011.

Kroll, J. H. and Seinfeld, J. H.: Chemistry of secondary organic aerosol: Formation and evolution of low-volatility organics in the atmosphere, Atmos. Environ., 42(16), 3593-3624, http://dx.doi.org/10.1016/j.atmosenv.2008.01.003, 2008.

Kroll, J. H., Smith, J. D., Che, D. L., Kessler, S. H., Worsnop, D. R. and Wilson, K.R.: Measurement of fragmentation and functionalization pathways in the heterogeneous oxidation of oxidized organic aerosol, Phys. Chem. Chem. Phys., 11(36), 8005-8014, doi:10.1039/b905289e, 2009.

Kuwata, M., Zorn, S. R. and Martin, S. T.: Using elemental ratios to predict the density of organic material composed of carbon, hydrogen, and oxygen, Environ. Sci. Technol., 46(2), 787-794, doi:10.1021/es202525q, 2011.

Lambe, A. T., Chhabra, P. S., Onasch, T. B., Brune, W. H., Hunter, J. F., Kroll, J. H., Cummings, M. J., Brogan, J. F., Parmar, Y., Worsnop, D. R., Kolb, C. E., and Davidovits, P.: Effect of oxidant concentration, exposure time, and seed particles on secondary organic aerosol chemical composition and yield, Atmos. Chem. Phys., 15(6), 3063-3075, doi:10.5194/acp-15-3063-2015, 2015.

Liggio, J., Li, S.-M., McLaren, R.: Heterogeneous reactions of glyoxal on particulate matter: Identification of acetals and sulfate esters, Environ. Sci. Technol., 39(6), 1532-1541, doi:10.1021/es048375y, 2015a.

Liggio, J., Li, S.-M., McLaren, R.: Reactive uptake of glyoxal by particulate matter. J. Geophys. Res.-Atmos., 110, D10304, doi:10.1029/2004JD005113, 2015b.

Li. L, Tang P., Nakao. S., and Cocker III, D. R..: Impact of Molecular Structure on Secondary Organic Aerosol Formation from Aromatic Hydrocarbon Photooxidation under Low NOx Conditions, –Atmos. Chem. Phys. Discuss, ~~under review,~~ 2015.

Lim, Y. B. and Ziemann, P. J.: Effects of molecular structure on aerosol yields from OH radical-initiated reactions of linear, branched, and cyclic alkanes in the presence of NO_x, Environ. Sci. Technol., 43(7), 2328-2334, doi:10.1021/es803389s, 2009a.

Lockhart, J., Blitz, M., Heard, D., Seakins, P. and Shannon, R.: Kinetic study of the OH+ glyoxal reaction: experimental evidence and quantification of direct OH recycling, J. Phys. Chem. A., 117(43), 11027-11037, doi:10.1021/jp4076806, 2013.

Loza, C. L., Chhabra, P. S., Yee, L. D., Craven, J. S., Flagan, R. C. and Seinfeld, J. H.: Chemical aging of *m*-xylene secondary organic aerosol: laboratory chamber study, Atmos. Chem. Phys., 12(1), 151-167, doi:10.5194/acp-12-151-2012, 2012.

Malloy, Q. G., Nakao, S., Qi, L., Austin, R., Stothers, C., Hagino, H. and Cocker III, D. R.: Real-Time Aerosol Density Determination Utilizing a Modified Scanning Mobility Particle Sizer—Aerosol Particle Mass Analyzer System, Aerosol Sci. Tech., 43(7), 673-678.doi:10.1080/02786820902832960, 2009.

Martín-Reviejo, M. and Wirtz, K.: Is benzene a precursor for secondary organic aerosol? Environ. Sci. Technol., 39(4), 1045-1054, doi:10.1021/es049802a, 2005.

Matsunaga, A., Docherty, K. S., Lim, Y. B. and Ziemann, P. J.: Composition and yields of secondary organic aerosol formed from OH radical-initiated reactions of linear alkenes in the presence of NO_x: Modeling and measurements, Atmos. Environ., 43(6), 1349-1357, doi:10.1016/j.atmosenv.2008.12.004, 2009.

McLafferty, F.W. and Tureček, F.: Interpretation of mass spectra. Univ Science Books, Sausalito, CA, USA, 1993.

Nakao, S., Clark, C., Tang, P., Sato, K. and Cocker III, D. R.: Secondary organic aerosol formation from phenolic compounds in the absence of NO_x, Atmos. Chem. Phys, 11, 10649-10660, doi:10.5194/acp-11-10649-2011, 2011.

Nakao, S., Liu, Y., Tang, P., Chen, C.-L., Zhang, J. and Cocker III, D. R.: Chamber studies of SOA formation from aromatic hydrocarbons: observation of limited glyoxal uptake, Atmos. Chem. Phys., 12(9), 3927-3937, doi:10.5194/acp-12-3927-2012, 2012.

Nakao, S., Tang, P., Tang, X., Clark, C. H., Qi, L., Seo, E., Asa-Awuku, A. and Cocker III, D. R.: Density and elemental ratios of secondary organic aerosol:

Application of a density prediction method, Atmos. Environ., 68, 273-277,doi:10.1016/j.atmosenv.2012.11.006, 2013.

Ng, N. L., Canagaratna, M. R., Jimenez, J. L., Chhabra, P. S., Seinfeld, J. H. and Worsnop, D. R.: Changes in organic aerosol composition with aging inferred from aerosol mass spectra, Atmos. Chem. Phys, 11(13), 6465-6474, doi:10.5194/acp-11-6465-2011, 2011.

Ng, N. L., Canagaratna, M. R., Zhang, Q., Jimenez, J. L., Tian, J., Ulbrich, I. M., Kroll, J. H., Docherty, K. S., Chhabra, P. S., Bahreini, R., Murphy, S. M., Seinfeld, J. H., Hildebrandt, L., Donahue, N. M., DeCarlo, P. F., Lanz, V. A., Prévôt, A. S. H., Dinar E., Rudich Y. and Worsnop D. R.: Organic aerosol components observed in Northern Hemispheric datasets from Aerosol Mass Spectrometry, Atmos. Chem. Phys., 10(10), 4625-4641, doi:10.5194/acp-10-4625-2010, 2010.

Ng, N. L., Kroll, J. H., Chan, A. W. H., Chhabra, P. S., Flagan, R. C. and Seinfeld, J. H.: Secondary organic aerosol formation from *m*-xylene, toluene, and benzene, Atmos. Chem. Phys., 7(14), 3909-3922, doi: 10.5194/acp-7-3909-2007, 2007.

Noziere, B., Dziedzic, P. and Córdova, A.: Products and kinetics of the liquid-phase reaction of glyoxal catalyzed by ammonium ions (NH_4^+), J. Phys. Chem. A., 113(1), 231-237, doi:10.1021/jp8078293, 2008.

Odum, J. R., Hoffmann, T., Bowman, F., Collins, D., Flagan, R. C. and Seinfeld, J. H.: Gas/particle partitioning and secondary organic aerosol yields, Environ. Sci. Technol., 30(8), 2580-2585, doi:10.1021/es950943+, 1996.

Odum, J. R., Jungkamp, T., Griffin, R., Flagan, R. C. and Seinfeld, J. H.: The atmospheric aerosol-forming potential of whole gasoline vapor, Science, 276(5309), 96-99, doi:10.1126/science.276.5309.96, 1997a.

Odum, J. R., Jungkamp, T., Griffin, R. J., Forstner, H., Flagan, R. C. and Seinfeld, J.H.: Aromatics, reformulated gasoline, and atmospheric organic aerosol formation, Environ. Sci. Technol., 31(7), 1890-1897, doi:10.1021/es960535l, 1997b.

Pang, Y., Turpin, B. and Gundel, L.: On the importance of organic oxygen for understanding organic aerosol particles, Aerosol Sci. Tech., 40(2), 128-133, doi:10.1080/02786820500423790, 2006.

Pankow, J. F. and Asher, W. E.: SIMPOL. 1: a simple group contribution method for predicting vapor pressures and enthalpies of vaporization of multifunctional organic compounds, Atmos. Chem. Phys., 8(10), 2773-2796, doi:10.5194/acp-8-2773-2008, 2008.

Pfaffenberger, L., Barmet, P., Slowik, J. G., Praplan, A. P., Dommen, J., Prévôt, A. S. H. and Baltensperger, U. : The link between organic aerosol mass loading and degree of oxygenation: an α-pinene photooxidation study, Atmos. Chem. Phys., 13(13), 6493-6506, doi:10.5194/acp-13-6493-2013, 2013.

Hassoun, S., Pilling, M. J. and Bartle, K. D.: A catalogue of urban hydrocarbons for the city of Leeds: atmospheric monitoring of volatile organic compounds by thermal desorption-gas chromatography, J. Environ. Monitor., 1(5), 453-458, doi:10.1039/a904879k, 1999.

Plum, C. N., Sanhueza, E., Atkinson, R., Carter, W. P. and Pitts, J. N.: Hydroxyl radical rate constants and photolysis rates of alpha-dicarbonyls, Environ. Sci. Technol., 17(8), 479-484, doi:10.1021/es00114a008, 1983.

Qi, L., Nakao, S., Malloy, Q., Warren, B. and Cocker, D. R.: Can secondary organic aerosol formed in an atmospheric simulation chamber continuously age? Atmos. Environ., 44(25), 2990-2996, doi:10.1016/j.atmosenv.2010.05.020, 2010a.

Qi, L., Nakao, S., Tang, P. and Cocker III, D. R.: Temperature effect on physical and chemical properties of secondary organic aerosol from *m*-xylene photooxidation, Atmos. Chem. Phys., 10(8), 3847-3854, doi:10.5194/acp-10-3847-2010, 2010b.

Rader, D. J. and McMurry, P. H.: Application of the tandem differential mobility analyzer to studies of droplet growth or evaporation, J. Aerosol. Sci., 17(5), 771-787, doi:10.1016/0021-8502(86)90031-5, 1986.

Salo, K., Hallquist, M., Jonsson, Å.M., Saathoff, H., Naumann, K.-H., Spindler, C., Tillmann, R., Fuchs, H., Bohn, B., Rubach, F., Mentel, T. F., Müller, L., Reinnig, M., Hoffmann, T., and Donahue, N. M.: Volatility of secondary organic aerosol during OH radical induced ageing, Atmos. Chem. Phys., 11(21), 11055-11067, doi:10.5194/acp-11-11055-2011, 2011.

Salter, R. J., Blitz, M. A., Heard, D. E., Kovács, T., Pilling, M. J., Rickard, A. R. and Seakins, P.W.: Quantum yields for the photolysis of glyoxal below 350 nm and parameterisations for its photolysis rate in the troposphere, Phys. Chem. Chem. Phys., 15(14), 4984-4994, doi:10.1039/c3cp43597k, 2013.

Sato, K., Hatakeyama, S. and Imamura, T.: Secondary organic aerosol formation during the photooxidation of toluene: NO_x dependence of chemical composition, J. Phys. Chem. A., 111(39), 9796-9808, doi:10.1021/jp071419f, 2007.

Sato, K., Takami, A., Isozaki, T., Hikida, T., Shimono, A. and Imamura, T.: 2010. Mass spectrometric study of secondary organic aerosol formed from the

photo-oxidation of aromatic hydrocarbons, Atmos. Environ., 44(8), 1080-1087, doi:10.1016/j.atmosenv.2009.12.013, 2010.

Sato, K., Takami, A., Kato, Y., Seta, T., Fujitani, Y., Hikida, T., Shimono, A. and Imamura, T. 2012. AMS and LC/MS analyses of SOA from the photooxidation of benzene and 1, 3, 5-trimethylbenzene in the presence of NO_x: effects of chemical structure on SOA aging, Atmos. Chem. Phys, 12, 4667-4682, doi:10.5194/acp-12-4667-2012, 2012.

Shilling, J. E., Chen, Q., King, S. M., Rosenoern, T., Kroll, J. H., Worsnop, D. R., DeCarlo, P. F., Aiken, A. C., Sueper, D., Jimenez, J. L. and Martin, S. T.: Loading-dependent elemental composition of α-pinene SOA particles, Atmos. Chem. Phys., 9(3), 771-782, doi:10.5194/acp-9-771-2009, 2009.

Singh, H.B., Salas, L., Viezee, W., Sitton, B. and Ferek, R.: 1992. Measurement of volatile organic chemicals at selected sites in California, Atmos. Environ. A-Gen., 26(16), 2929-2946, doi:10.1016/0960-1686(92)90285-S, 1992.

Singh, H. B., Salas, L. J., Cantrell, B. K. and Redmond, R. M.: Distribution of aromatic hydrocarbons in the ambient air, Atmos. Environ. (1967), 19(11), 1911-1919, doi:10.1016/0004-6981(85)90017-4, 1985.

Song, C., Na, K. and Cocker III, D. R.: Impact of the hydrocarbon to NO_x ratio on secondary organic aerosol formation, Environ. Sci. Technol., 39(9), 3143-3149, doi:10.1021/es0493244, 2005.

Takegawa, N., Miyakawa, T., Kawamura, K. and Kondo, Y.: Contribution of selected dicarboxylic and ω-oxocarboxylic acids in ambient aerosol to the m/z 44 signal of an Aerodyne aerosol mass spectrometer, Aerosol Sci. Tech., 41(4), 418-437, doi:10.1080/02786820701203215, 2007.

Takekawa, H., Minoura, H. and Yamazaki, S.: Temperature dependence of secondary organic aerosol formation by photo-oxidation of hydrocarbons, Atmos. Environ., 37(24), 3413-3424, doi:10.1016/S1352-2310(03)00359-5, 2003.

Tkacik, D. S., Presto, A. A., Donahue, N. M. and Robinson, A. L.: Secondary organic aerosol formation from intermediate-volatility organic compounds: cyclic, linear, and branched alkanes, Environ. Sci. Technol., 46(16), 8773-8781, doi:10.1021/es301112c, 2012.

Tritscher, T., Dommen, J., DeCarlo, P. F., Gysel, M., Barmet, P. B., Praplan, A. P., Weingartner, E., Prévôt, A. S. H., Riipinen, I., Donahue, N. M. and Baltensperger, U.:

Volatility and hygroscopicity of aging secondary organic aerosol in a smog chamber, Atmos. Chem. Phys., 11(22), 11477-11496, doi:10.5194/acp-11-11477-2011, 2011.

Võ, U.-U.T. and Morris, M.P.: Nonvolatile, semivolatile, or volatile: Redefining volatile for volatile organic compounds. Journal of the Air & Waste Management Association, 64(6), 661-669, doi: 10.1080/10962247.2013.873746, 2014.

Wyche, K. P., Monks, P. S., Ellis, A. M., Cordell, R. L., Parker, A. E., Whyte, C., Metzger, A., Dommen, J., Duplissy, J., Prevot, A. S. H., Baltensperger, U., Rickard, A. R., and Wulfert, F.: Gas phase precursors to anthropogenic secondary organic aerosol: detailed observations of 1, 3, 5-trimethylbenzene photooxidation, Atmos. Chem. Phys., 9(2), 635-665, doi:10.5194/acp-9-635-2009, 2009.

Xiang, B., Zhu, L. and Tang, Y.: Photolysis of 4-Oxo-2-pentenal in the 190-460 nm Region, J. Phys. Chem. A., 111(37), 9025-9033, doi:10.1021/jp0739972, 2007.

Yu, J., Jeffries, H. E. and Sexton, K. G. 1997. Atmospheric photooxidation of alkylbenzenes—I. Carbonyl product analyses, Atmos. Environ., 31(15), 2261-2280, doi:10.1016/S1352-2310(97)00011-3, 1997.

Yu, L., Smith, J., Laskin, A., Anastasio, C., Laskin, J., Zhang, Q.: Chemical characterization of SOA formed from aqueous-phase reactions of phenols with the triplet excited state of carbonyl and hydroxyl radical, Atmos. Chem. Phys., 14(24), 13801-13816, doi:10.5194/acp-14-13801-2014, 2014.

Zhang, Q., Alfarra, M. R., Worsnop, D. R., Allan, J. D., Coe, H., Canagaratna, M. R. and Jimenez, J. L.: Deconvolution and quantification of hydrocarbon-like and oxygenated organic aerosols based on aerosol mass spectrometry, Environ. Sci. Technol., 39(13), 4938-4952, doi:10.1021/es048568l, 2005.

Ziemann, P.: Effects of molecular structure on the chemistry of aerosol formation from the OH-radical-initiated oxidation of alkanes and alkenes, International Reviews in Physical Chemistry, 30(2), 161-195, doi:10.1080/0144235X.2010.550728, 2011.

Table 1. Experiment conditions*

Precursor	ID	HC/NO[a]	NO[b]	HC[b]	ΔHC[c]	M_0[c]	Yield
Benzene	1223A	98.1	59.5	972	398	139	0.35
	1223B	49.3	119	979	453	105	0.23
	1236A	104	53.6	928	407	106	0.26
	1236B	36.4	154	938	450	34.9	0.08
	1237A	62.7	41.6	435	266	45.9	0.17
	1237B	129	21.1	453	253	51.4	0.20
	1618A	102	35.4	603	354	46.3	0.13
Toluene	1101A	29.0	19.2	79.7	206	30.1	0.15
	1101B	58.8	9.40	78.8	176	25.1	0.14
	1102A	12.2	43.3	75.7	223	21.8	0.10
	1102B	17.5	33.0	82.5	238	22.2	0.09
	1106A	13.2	20.1	38.0	126	9.80	0.08
	1106B	24.4	10.6	36.9	111	12.4	0.11
	1468A	26.1	64.1	239	667	130	0.20
	1468B	26.5	63.0	238	671	127	0.19
m-Xylene	1191A	12.6	52.2	82.1	298	15.2	0.05
	1191B	14.6	45.7	83.6	340	14.6	0.04
	1193A	15.5	36.8	71.1	239	13.6	0.06
	1193B	15.2	36.5	69.5	236	11.2	0.05
	1191A	12.6	52.2	82.1	298	15.2	0.05
	1191B	14.6	45.7	83.6	340	14.6	0.04
	1516A	27.8	26.7	92.9	357	48.7	0.14
	1950A	14.1	45.5	80.0	327	26.3	0.08
	1950B	14.6	45.9	83.6	345	28.7	0.08
1,2,4-Trimethylbenzene	1117A	69.8	10.3	80.0	335	16.8	0.05
	1117B	34.8	20.7	80.0	368	18.2	0.05
	1119A	14.1	49.8	78.0	385	19.6	0.05
	1119B	17.1	41.6	79.0	390	25.5	0.07
	1123A	71.0	10.1	80.0	300	11.2	0.04
	1123B	32.6	22.1	80.0	345	15.4	0.05
	1126A	69.3	10.1	77.5	286	12.6	0.04
	1126B	28.1	24.3	75.9	333	15.4	0.05
	1129B	24.2	15.6	42.0	201	5.60	0.03
1,2,4,5-Tetramethylbenzene	1531A	72.0	25.0	180	752	17.9	0.02
	1603A	109	11.2	122	469	3.12	0.01
	1603B	110	11.1	123	464	2.54	0.01
	2085A	60.6	33.4	202	862	29.2	0.03
	2085B	136	12.9	175	502	8.20	0.02
Pentamethylbenzene	1521A	68.8	23.5	147	893	32.7	0.04
	1627A	77.9	20.0	142	769	20.6	0.03
	1627B	26.6	50.0	121	719	24.8	0.03
Hexamethylbenzene	1557A	72.0	28.0	168	999	23.4	0.02
	2083A	78.4	11.6	76.0	442	15.2	0.03
	2083B	41.3	22.0	76.0	483	14.0	0.03

Note: a) Unit of HC/NO are ppbC:ppb; b)Unit of NO and HC are ppb; c)Unit of Δ HC and M_0 are $\mu g \cdot m^{-3}$, M_0 is a wall loss and density corrected particle mass concentration; * Only newly added data are listed here and published data are listed in Table S2.

Table 2. Two product yield curve fitting parameters

Yield Curve	α_1	$K_{om,1}$ (m^3/μg)	α_2	$K_{om,2}$ (m^3/μg)
Benzene	0.082	0.017	0.617	0.005
Toluene	0.185	0.080	0.074	0.005
m-Xylene	0.148	0.047	0.079	0.005
1,2,4-Trimethylbenzene	0.099	0.047	0.079	0.005
C_{10+}	0.048	0.047	0.065	0.005

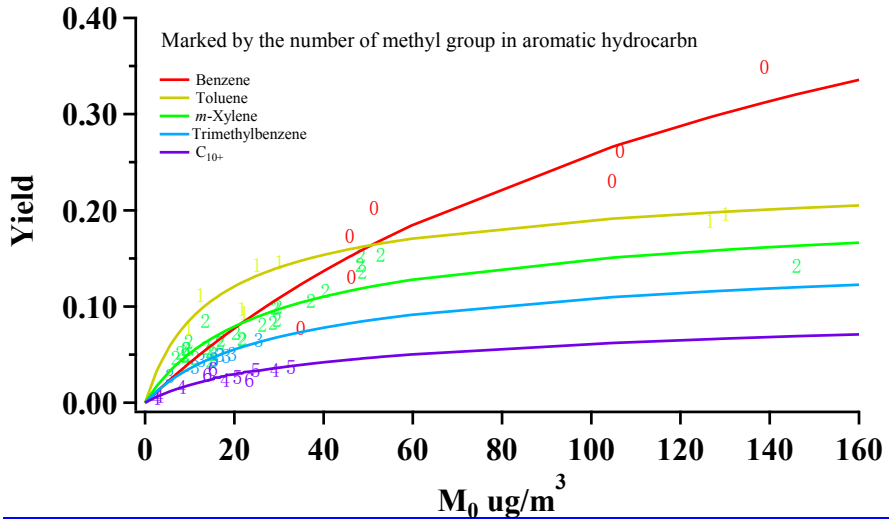

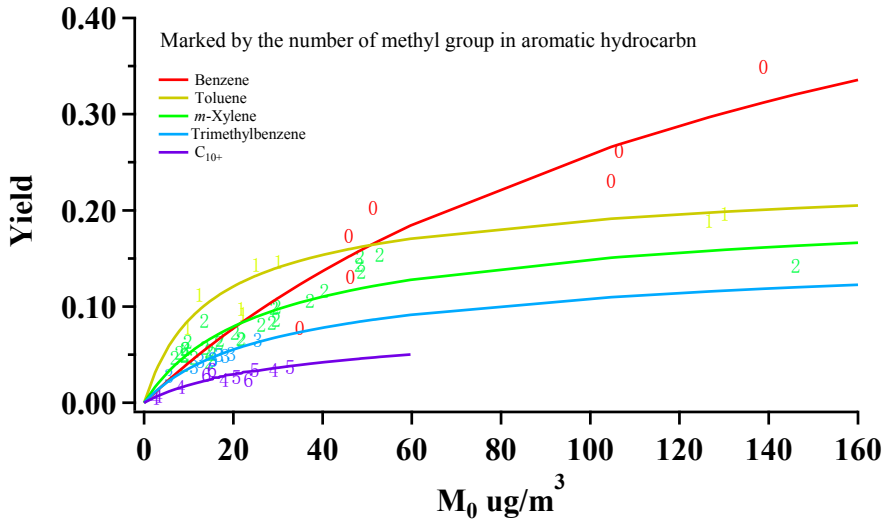

Formatted: Right

Fig. 1. Aromatic SOA yields as a function of M_0 *Note: Song, et al. (2005) *m*-xylene data are also included

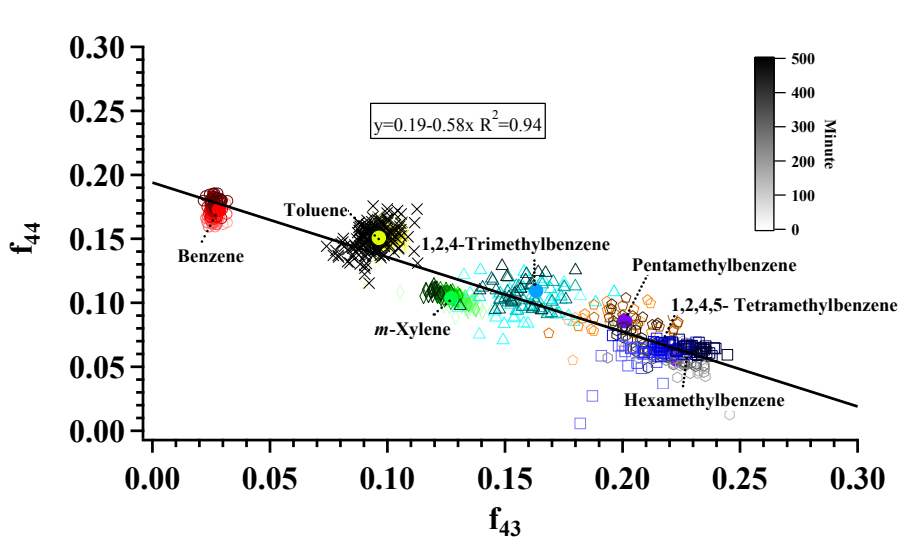

Fig. 2. f_{44} and f_{43} evolution in SOA formed from photooxidation of different monocyclic aromatic hydrocarbons under low NO_x (Benzene 1223A; Toluene 1468A; *m*-Xylene 1950A; 1,2,4-Trimethylbenzene 1119A; 1,2,4,5-Tetramethylbenzene 2085A; Pentamethylbenzene 1627A; Hexamethylbenzene 2083A; colored solid circle markers represent the location of average f_{44} and f_{43} value during photooxidation)

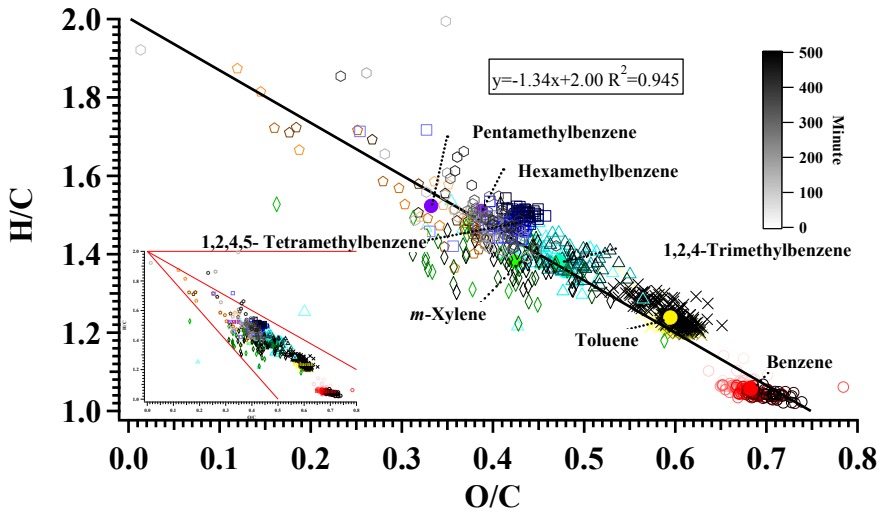

(a)

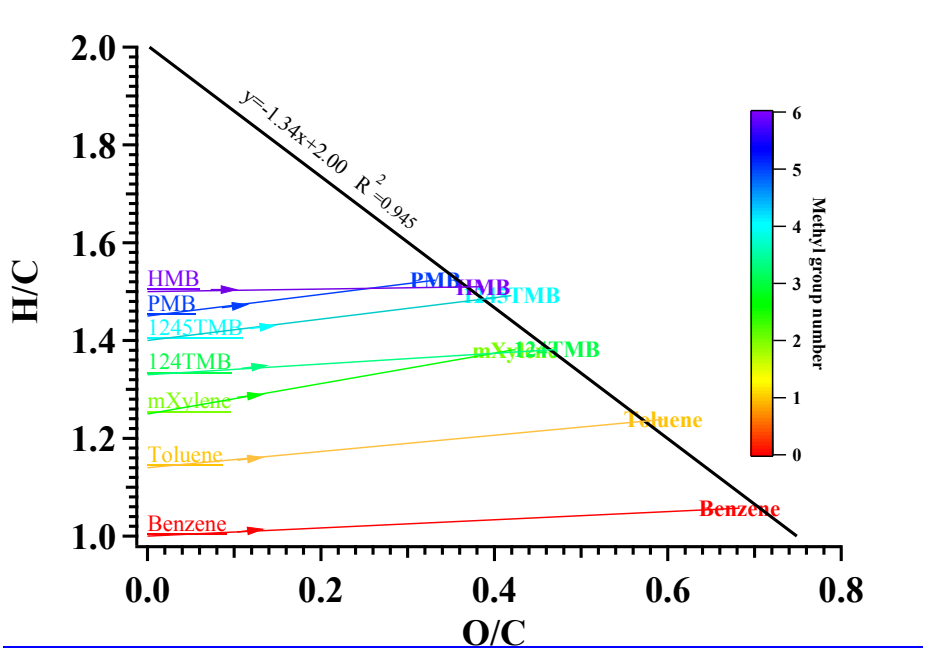

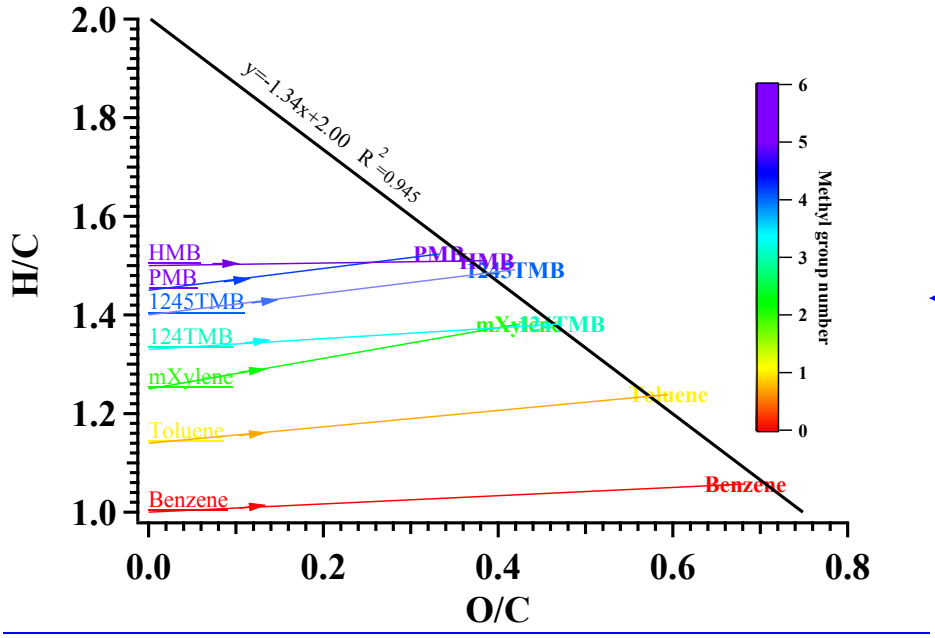

(b)

Fig. 3. a) H/C and O/C evolution; the inset graph shows the measured values relative to the classic triangle plot (Ng et al., 2010). b) Average H/C and O/C in SOA formed from monocyclic aromatic hydrocarbon photooxidation under low NO_x (Benzene

Formatted: Centered

1223A; Toluene 1468A; *m*-Xylene 1191A; 1,2,4-Trimethylbenzene 1119A; 1,2,4,5-Tetramethylbenzene 2085A; Pentamethylbenzene 1627A; Hexamethylbenzene 2083A).

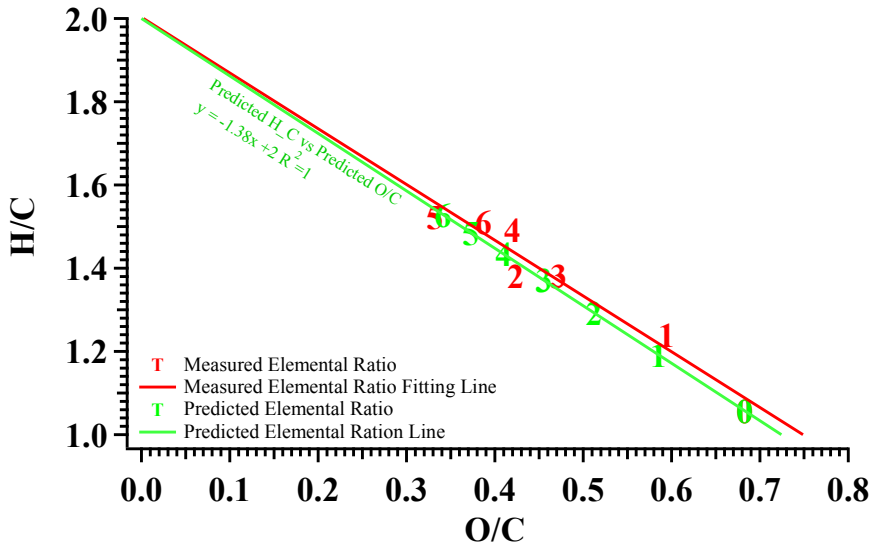

(a)

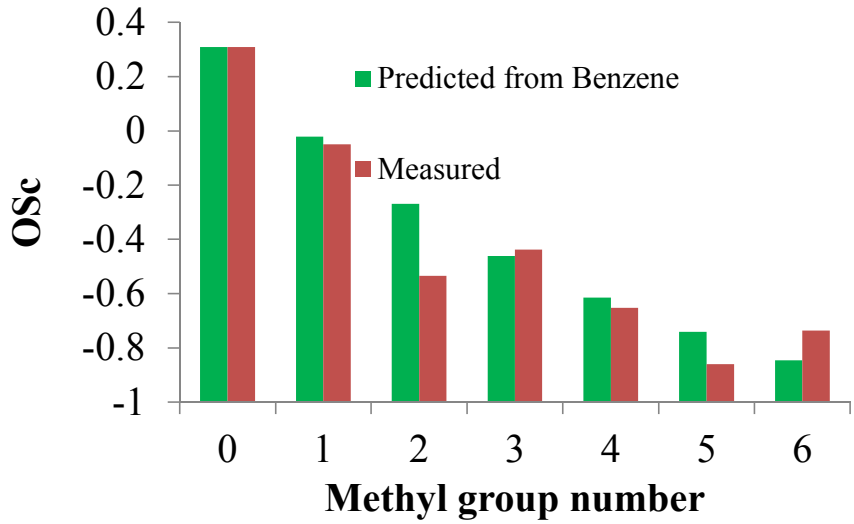

(b)

Fig. 4. Comparison of predicted and measured O/C (a), H/C (a) and oxidation state (OSc) (b) in SOA formation from monocyclic aromatic hydrocarbon photooxidation under low NO_x (Benzene 1223A; Toluene 1468A; m-Xylene 1191A; 1, 2, 4-Trimethylbenzene 1119A; 1,2,4,5-Tetramethylbenzene 1306A; Pentamethylbenzene 1627A; Hexamethylbenzene 1557A)

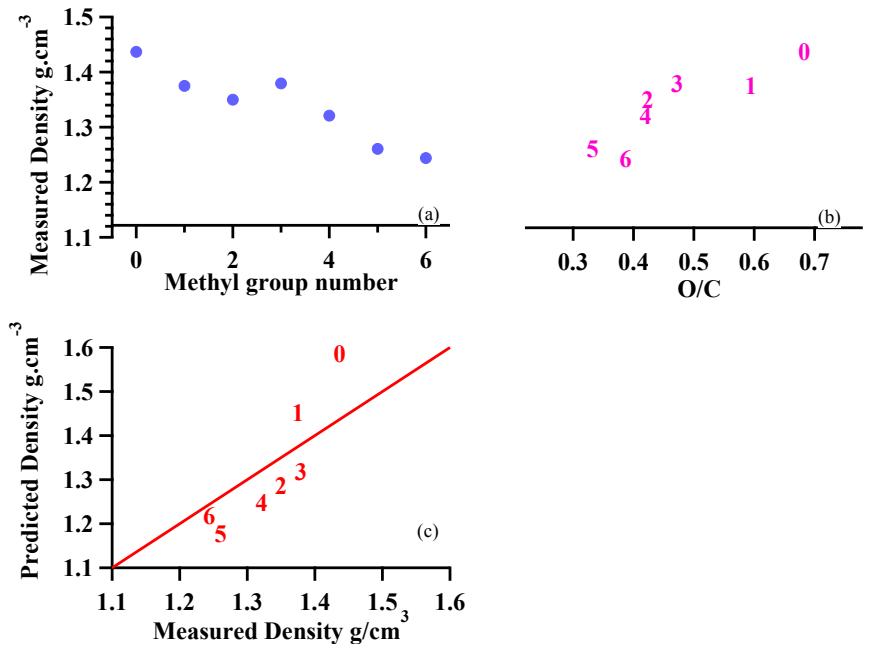

Fig. 5. Relationship between (a) SOA density and methyl group number; (b) SOA density and O/C; (c) predicted and measured density from monocyclic aromatic hydrocarbon photooxidation under low NO_x (number mark represents number of methyl groups on aromatic hydrocarbon ring)

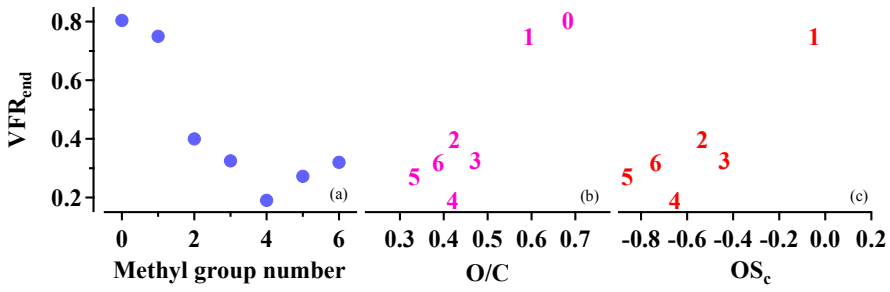

Fig. 6. Relationship between a) SOA volatility and methyl group number; b) SOA volatility and O/C; c) SOA volatility and oxidation state (OS_c) from monocyclic aromatic hydrocarbon photooxidation under low NO_x (number mark represents number of methyl groups on aromatic hydrocarbon ring).

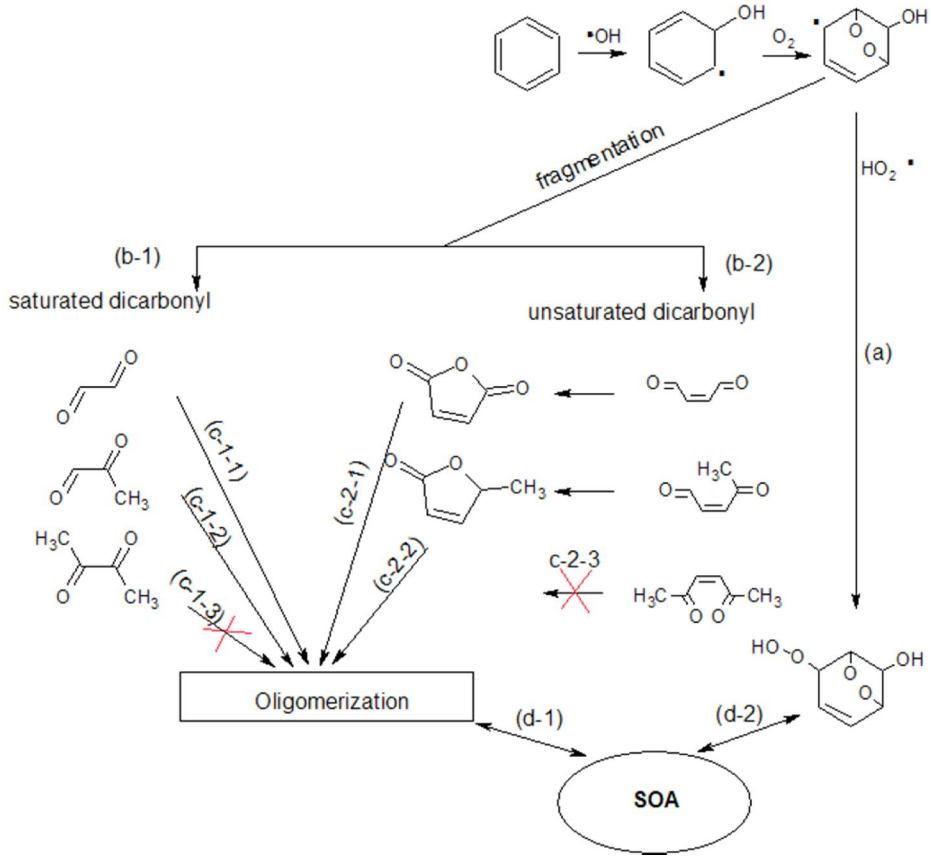

Fig. 7. Monocyclic ~~Aromatic~~ aromatic hydrocarbon oxidation pathways related to SOA formation (~~benzene shown as an example~~methyl substitute on aromatic ring not shown)

Aromatic Hydrocarbon + OH → S_1^g → S_2^g → S_3^g

↓ ↑ ↓ ↑

S_1^p S_3^p

Fig. 8. Kinetic scheme for SOA formation from monocyclic aromatic hydrocarbon

Formatted: Indent: First line: 14.5 ch

Formatted: Font: (Asian) SimSun

Table S1 Aromatic hydrocarbon physical properties and rate constant

Compound	Vapor Pressure[a]	Boiling Point[b]	k_{OH}[c]	SAPRC-k_{OH}[d]
Benzene	75	80	0.139	0.122
Toluene	21	111	0.563	0.558
m-Xylene	9	139	2.31	2.31
1,2,4-trimethylbenzene	2.1	170	3.25	3.25
1,2,4,5-tetramethylbenzene	5.28E-1	193	5.55	4.10
Pentamethylbenzene	3.48E-02*	232	10.3	7.63
Hexamethylbenzene	8.60E-04	265	11.3	11.3

Note: a) vapor pressures are referred to Chemispider in unit mmHg at 25 °C; b) boiling points are referred to Chemispider in unit °C; c) OH reaction rate constants are refer to Calvert, et al, 2002; Atkinson and Arey, 2003; Aschmann, et al, 2013 in unit 10^{-11} cm^3 $molecule^{-1}$ s^{-1} at 25 °C. d) OH reaction rate constants used in SAPRC-11 model in unit 10^{-11} cm^3 $molecule^{-1}$ s^{-1} at 25 °C ; * Experimental vapor pressure measured at 20°C, An estimated vapor pressure at 25°C is 3.56e-2 according to Chemispider. ~~Predicted data from Chemispider~~.

Table S2 Experimental conditions for additional *m*-xylene experiments from Song, et al. (2005)

ID	HC/NO[a]	NO[b]	HC[b]	ΔHC[c]	M_0[c]	Yield
104A	10.1	64.4	81.3~~350~~	328	21.7	0.07
104B	29.3	21.4	78.4~~338~~	281	20.4	0.07
107A	26.0	89.6	291~~1254~~	1029	146	0.14
129A	15.1	45.5	86~~371~~	336	21.9	0.07
149A	13.3	50.2	83.6~~360~~	342	52.8	0.15
164A	12.4	44.0	68.0~~293~~	271	16.8	0.06
164B	12.2	44.1	67.5~~291~~	270	14.6	0.05
217A	36.8	8.90	40.9~~176~~	155	9.80	0.06
217B	35.9	8.70	39~~168~~	153	7.90	0.05
219A	63.7	7.00	55.7~~240~~	165	9.20	0.06
219B	67.5	6.60	55.7~~240~~	166	9.30	0.06
288A	63.1	7.00	55.2~~238~~	183	9.00	0.05
290A	31.1	15.3	59.5~~256~~	229	9.00	0.04
293A	29.9	13.7	51.2~~221~~	189	9.20	0.05
368A	17.9	21.0	47.0~~203~~	149	6.90	0.05
485A	17.5	43.3	94.7~~408~~	353	37.2	0.11
485B	16.7	45.0	93.7~~404~~	349	40.4	0.12
488A	15.5	46.2	89.6~~386~~	341	29.5	0.09
492A	13.6	44.3	75.2~~324~~	296	29.1	0.10
492B	13.5	44.8	75.5~~325~~	298	29.7	0.10
566A	14.0	48.3	84.5~~364~~	337	48.2	0.14
566B	13.3	48.0	79.8~~344~~	318	48.4	0.15
758A	47.5	11.4	67.7~~292~~	158	13.5	0.09
820A	30.2	20.7	78.1~~337~~	260	17.0	0.07

Note: a) Unit of HC/NO are ppbC:ppb; b) Unit of NO and HC are ppb; c) Unit of ΔHC and M_0 are $\mu g \cdot m^{-3}$

Table S3 Average radical concentrations throughout photooxidation

Run ID	RO_2[a]	HO_2[a]	OH[b]	HO_2*RO[c]	HO_2/RO_2	NO/HO_2	OH/HO_2[d]	NO_3[a]
1236A	12.9	23.5	4.9	530	2.7	4.9E+03	3.3E-02	1.8
1236B	1.30	4.4	4.7	30.4	3.9	5.9E+05	3.6E-01	8.3
1237A	15.2	20.8	7.6	488	2.3	3.1E+04	1.4E-01	1.9
1237B	13.7	20.7	5.6	416	2.3	2.3E+02	1.2E-02	0.9
1223A	10.5	24.0	4.7	376	2.7	1.5E+04	6.2E-02	1.7
1618A	9.50	107.2	5.5	1194	13.5	3.1E+01	1.1E-03	6.2
1223B	10.0	16.4	7.0	508	3.2	1.7E+08	4.3E+01	5.6
1101A	15.7	19.3	6.8	335	1.4	5.8E+01	7.8E-03	4.0
1101B	16.3	18.5	5.0	320	1.2	8.9E+00	3.8E-03	1.4
1102A	12.9	17.3	10	313	1.7	1.6E+04	1.2E-01	16.2
1102B	13.8	17.5	8.7	328	1.6	1.0E+03	2.8E-02	10.5
1106A	7.30	12.3	10	118	1.9	8.1E+02	3.9E-02	16.3
1106B	9.30	14.5	7.9	144	1.6	1.5E+01	8.2E-03	6.0
1468A	23.8	24.5	3.9	716	1.3	6.3E+01	3.2E-03	11.8
1468B	26.4	26.3	4.1	740	1.0	4.6E+01	3.1E-03	4.8
1193A	11.0	12.3	3.1	185	1.3	1.5E+06	1.8E+00	14.0
1193B	9.00	11.6	2.8	141	1.4	3.2E+05	4.2E-01	18.7
1191A	19.1	15.8	5.8	449	1.2	4.5E+05	3.4E-01	32.0
1191B	10.8	12.4	2.4	190	1.5	3.8E+04	5.1E-02	18.5
1516A	18.6	23.1	3.1	465	1.3	1.5E+01	2.0E-03	2.4
1950A	11.7	20.6	4.5	267	1.8	7.2E+01	4.3E-03	38.4
1950B	13.3	22.0	4.6	326	1.7	4.6E+01	3.7E-03	37.1
1117A	13.1	15.8	1.7	220	1.3	1.2E+01	1.5E-03	7.3
1117B	9.80	14.6	2.5	172	1.6	1.9E+02	4.7E-03	34.9
1119A	12.5	18.8	5.3	300	1.7	2.7E+03	1.7E-02	89.0
1119B	12.2	17.3	4.0	296	1.9	2.9E+03	1.7E-02	68.6
1123A	15.9	15.1	1.7	274	1.1	6.8E+01	2.2E-03	2.9
1123B	15.8	18.6	2.5	321	1.2	7.7E+01	3.0E-03	23.2
1126A	17.3	17.6	1.7	324	1.1	1.7E+01	1.5E-03	4.3
1126B	30.0	24.8	7.5	841	1.0	3.2E+01	3.8E-03	33.7
1129B	11.2	15.4	4.3	199	1.6	5.6E+01	4.9E-03	24.0
1531A	N/A	N/A	N/A	N/A	N/A	N/A	N/A	N/A
1603A	40.9	21.8	1.6	971	0.7	2.3E+01	9.5E-04	0.6
1603B	38.9	20.4	1.6	925	0.8	7.7E+01	1.3E-03	0.6

2085A	31.5	28.3	1.2	971.5	1.1	3.2E+01	6.7E-04	2.2
2085B	27.4	22.7	0.6	642.2	1.0	3.7E+00	3.2E-04	0.5
1488A	N/A	N/A	N/A	N/A	N/A	N/A	N/A	N/A
1521A	24.7	23.5	0.8	621	1.0	4.7E+01	5.4E-04	1.2
1627A	27.8	23.0	1.0	702	1.0	5.7E+01	6.9E-04	1.0
1627B	15.5	22.2	2.1	439	1.6	4.0E+03	4.9E-03	47.5
1557A	10.1	16.7	0.2	171	1.7	1.6E+00	9.3E-05	0.5
2083A	13.5	15.6	0.9	280	1.3	1.6E+06	6.0E-01	1.1
2083B	10.0	17.0	1.2	213	1.8	4.0E+02	2.0E-03	13.8

Note: average radical concentrations are calculated by dividing time integrated radical parameters with photooxidation time; average radical concentration throughout photooxidation a) in 10^6 molecules·cm^{-3}; b) in 10^8 molecules·cm^{-3}; c) in 10^{16}molecules·cm^{-3}; d) average radical ratio throughout photooxidation in 10^3

Table S4 Correlation between SOA yields and average radical concentrations

	RO_2	HO_2	OH	HO_2*RO_2	HO_2/ RO_2	NO/HO_2	OH/HO_2	NO_3
Yield	-0.243	0.169	0.459	0.067	0.261	0.294	0.292	-0.237
p-value[a]	0.125	0.292	0.003	0.678	0.099	0.062	0.064	0.136

Note: a) P-values range from 0 to 1, 0-reject null hypothesis and 1 accept null hypothesis. Alpha (α) level used is 0.05. If the p-value of a test statistic is less than alpha, the null hypothesis is rejected

Table S5 Correlation among SOA density, volatility (VFR), SOA chemical composition and methyl group number

	Density	VFR_{end}[a]	f_{44}	f_{43}	H/C	O/C	OS_c	Methyl[c]
Density	-	0.715	0.790	-0.839	-0.756	**0.873**	0.834	-0.943
p-value[b]	-	0.071	0.034	0.018	0.049	0.01	0.02	0.001
VFR_{end}[a]	0.715	-	0.768	-0.896	-0.905	**0.937**	0.932	-0.838
p-value[b]	0.071	-	0.044	0.006	0.005	0.002	0.002	0.0019

Note: a) VFR_{end} volume remaining fraction at the end of photooxidation; b) P-values range from 0 to 1, 0-reject null hypothesis and 1 accept null hypothesis. Alpha (α) level used is 0.05. If the p-value of a test statistic is less than alpha, the null hypothesis is rejected; c) Methyl group number is used for statistical analysis

Table S6 Vapor pressure predication of selected benzene photooxidation products

Formula	Reaction pathway	Predicted $logP_{vap}$[a]
$C_6H_6O_5$	S_1, Bicyclic peroxide	-3.83E+00

$C_6H_6O_8$	S_1,Bicyclic peroxide	-6.39E+00
$C_8H_{10}O_{10}$	S_3, Oligomerization, c-2-1	-1.13E+01
$C_8H_{10}O_9$	S_3, Oligomerization, c-1-1	-7.47E+00
$C_6H_8O_6$	S_3, Oligomerization, c-2-1, with glyoxal	-6.92E+00

Note : a) Prediction is based on Pankow and Asher 2008, $\log P_{vap}$ is in the unit of log(atm)

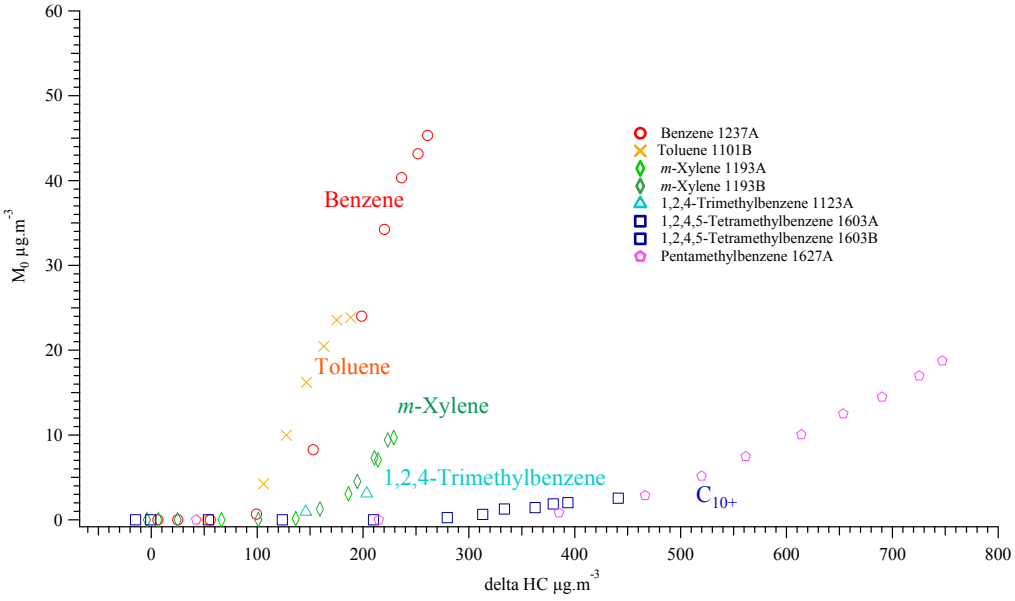

Fig. S1. Aromatic SOA growth curve (particle concentration M_0 vs. hydrocarbon consumption ΔHC)

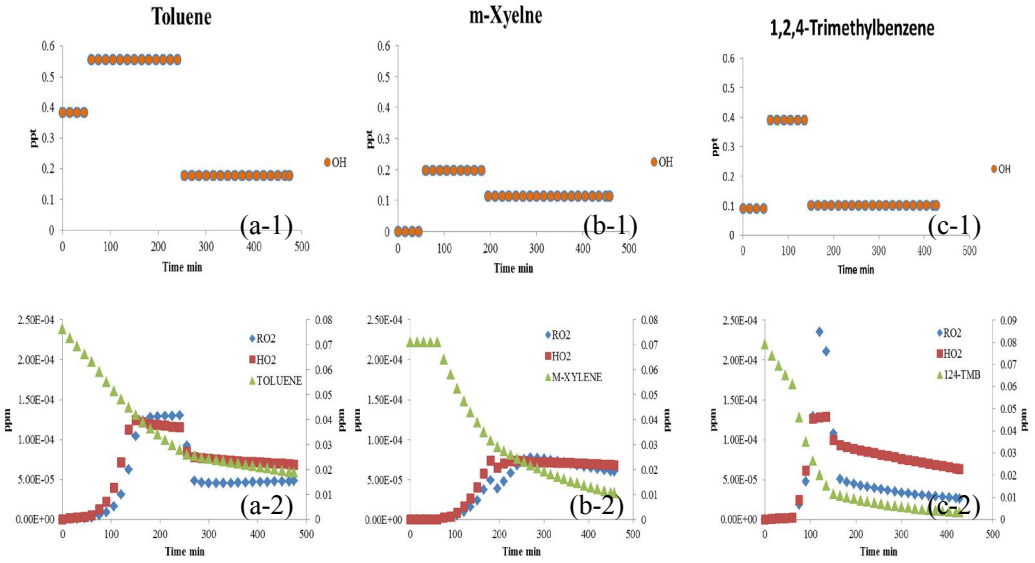

Fig. S2. Time series radical profile during photooxidation (a) toluene 1102B; (b) *m*-xylene 1193A; (c) 1,2,4-trimethylbenzene 1119B)

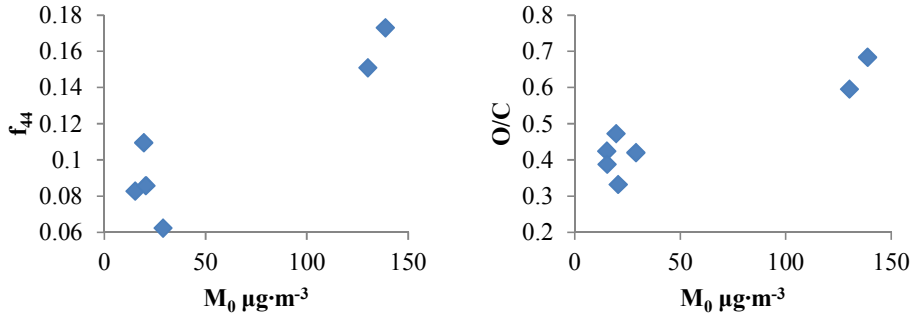

Fig.S3. Relationship between f_{44}, O/C and mass loading

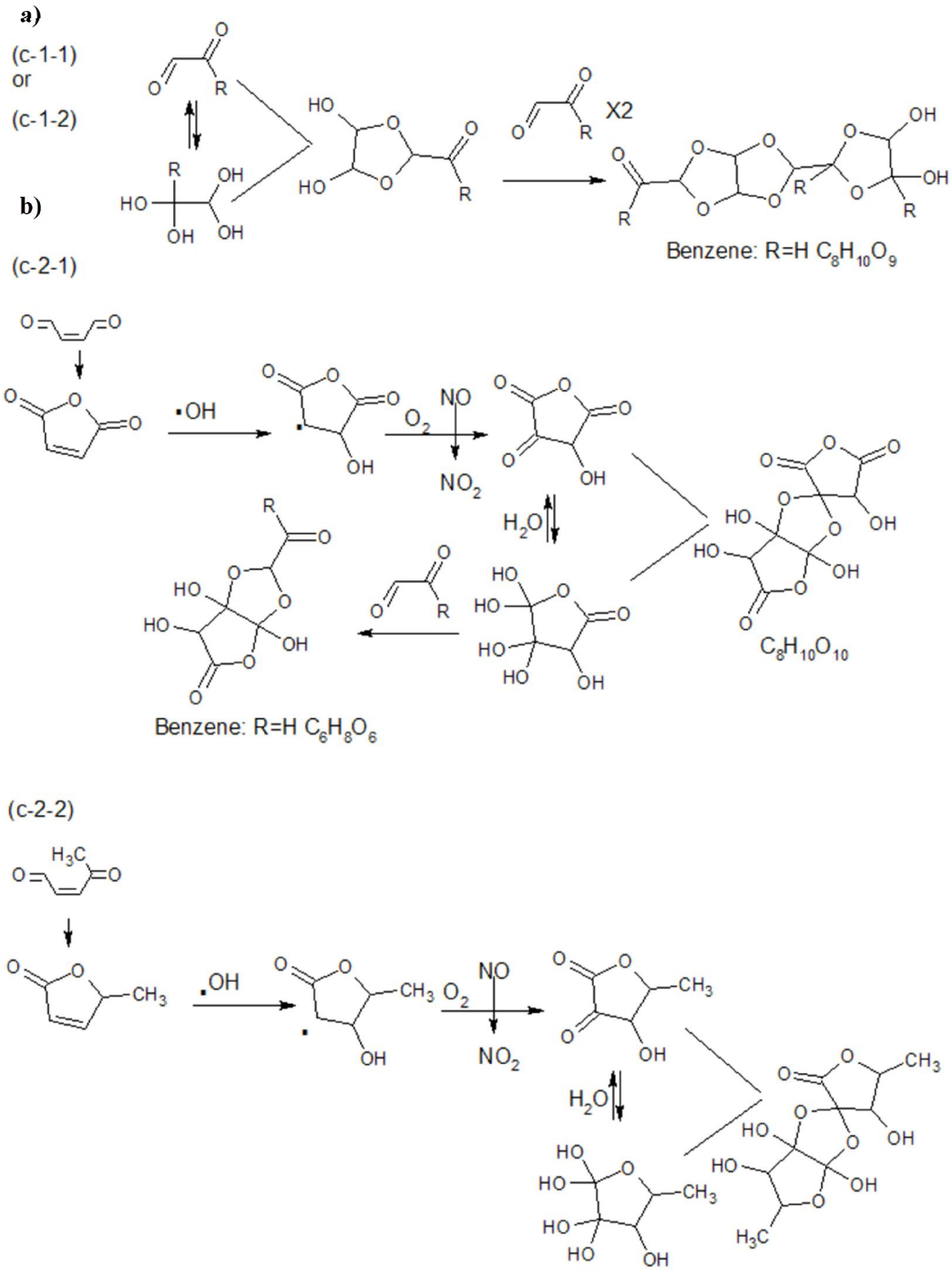

Fig. S4. Potential oligomerization pathways during aromatic hydrocarbon photooxidation a) from saturated 1,2-dicarbonyls to oligomers (adopted from Kalberer, et al, 2004); b) from unsaturated 1,4-dicarbonys to oligomers (c-1-1, c-1-2, c-2-1 and c-2-2 are pathways mentioned in Fig. 7.).

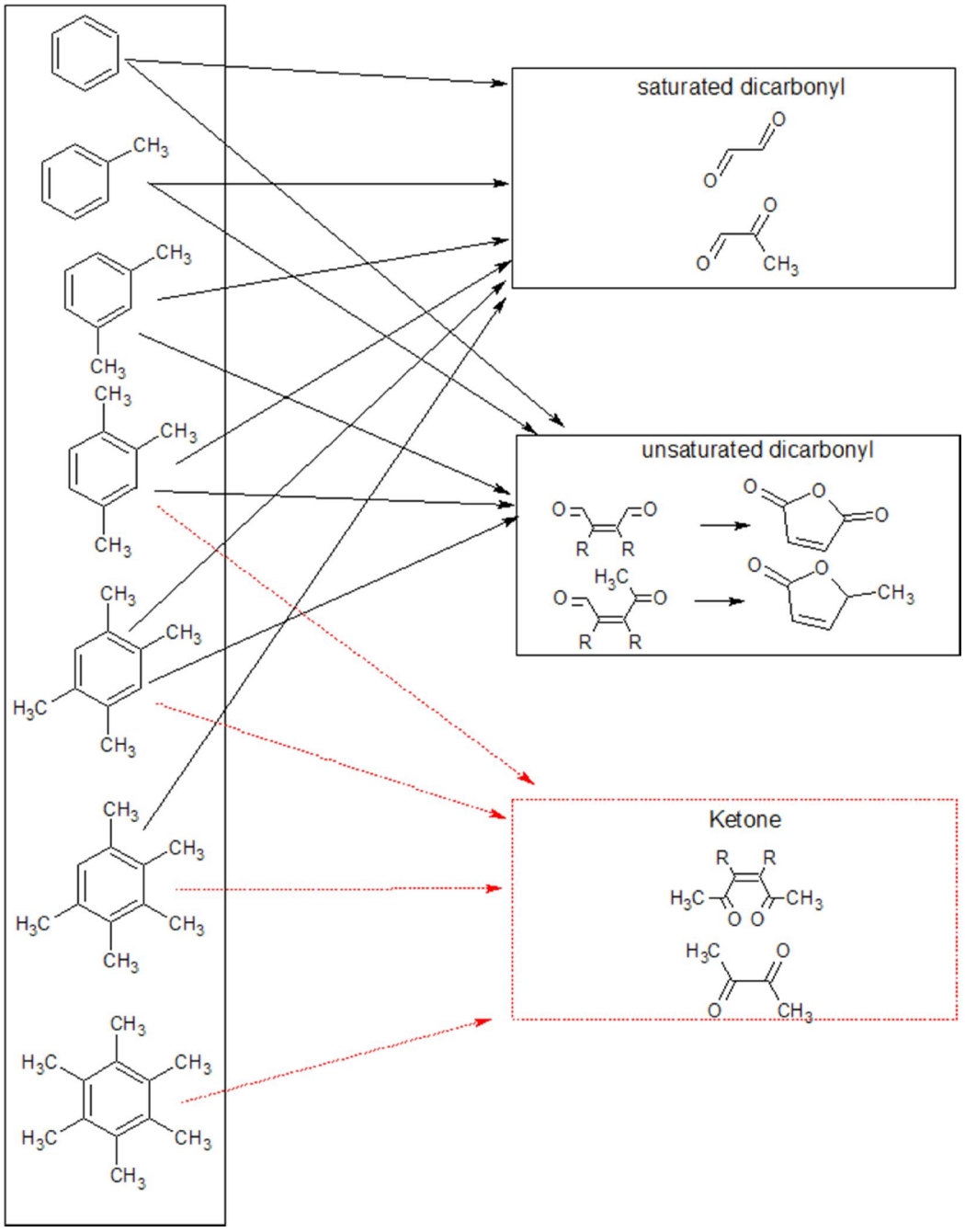

Fig S5. Potential ring opening products of aromatic hydrocarbons during photooxidation (OH attach to ring carbon not occupied by a methyl group is the only pathway considered in pentamethylbenzene photoxidation)